

# cGMP-Elevating Compounds and Ischemic Conditioning Provide Cardioprotection Against Ischemia and Reperfusion Injury via Cardiomyocyte-Specific BK Channels

**Running Title:** *Frankenreiter et al.; Cardiomyocyte-Specific BK Channels in I/R Injury*

Sandra Frankenreiter, Dr. rer. nat.<sup>1</sup>; Piotr Bednarczyk, Dr. hab.<sup>2</sup>; Angelina Kniess<sup>1</sup>;  
Nadja Bork, MSc<sup>3</sup>; Julia Straubinger, Dr. rer. nat.<sup>1</sup>; Piotr Koprowski, Dr. hab.<sup>4</sup>;  
Antoni Wrzosek, Dr.<sup>4</sup>; Eva Mohr, MSc<sup>1</sup>; Angela Logan, PhD<sup>5</sup>; Michael P. Murphy, PhD<sup>5</sup>;  
Meinrad Gawaz, Dr. med.<sup>6</sup>; Thomas Krieg, Dr. med.<sup>7</sup>; Adam Szewczyk, Dr. hab.<sup>4</sup>;  
Viacheslav O. Nikolaev, Dr. rer. nat.<sup>3</sup>; Peter Ruth, Dr. rer. nat.<sup>1</sup>; Robert Lukowski, Dr. rer. nat.<sup>1</sup>

<sup>1</sup>Department of Pharmacology, Toxicology and Clinical Pharmacy, Institute of Pharmacy, University of Tuebingen, Tuebingen, Germany; <sup>2</sup>Department of Biophysics, Warsaw University of Life Sciences, Warsaw, Poland; <sup>3</sup>Institute of Experimental Cardiovascular Research, University Medical Center Hamburg- Eppendorf, Hamburg, Germany; <sup>4</sup>Laboratory of Intracellular Ion Channels, Nencki Institute of Experimental Biology, Warsaw, Poland; <sup>5</sup>MRC Mitochondrial Biology Unit, University of Cambridge, Cambridge Biomedical Campus, Cambridge, UK; <sup>6</sup>Internal Medicine III, Cardiology and Cardiovascular Medicine, University Hospital Tuebingen, Tuebingen, Germany; <sup>7</sup>Department of Medicine, University of Cambridge, Cambridge Biomedical Campus, Cambridge, UK

## Address for Correspondence:

Robert Lukowski, Dr. rer. nat  
Department of Pharmacology, Toxicology and Clinical Pharmacy  
Institute of Pharmacy  
University of Tuebingen, Tuebingen, Germany  
Tel. +49 7071 29 74550  
Fax +49 7071 29 2476  
Email: robert.lukowski@uni-tuebingen.de

## Abstract

**Background**—The nitric oxide-sensitive guanylyl cyclase (NO-GC)/cyclic guanosine-3',5'-monophosphate (cGMP)/cGMP-dependent protein kinase type I (cGKI)-signaling pathway can afford protection against the ischemia and reperfusion (I/R) injury that occurs during myocardial infarction (MI). Reportedly, voltage and  $\text{Ca}^{2+}$ -activated  $\text{K}^{+}$  channels of the BK-type are stimulated by cGMP/cGKI and recent *ex-vivo* studies implicated that increased BK activity favors the survival of the myocardium at I/R. It remains unclear, however, whether the molecular events downstream of cGMP involve BK channels present in cardiomyocytes (CMs) or in other cardiac cell types.

**Methods**—Gene-targeted mice with a CM- or smooth muscle (SM) cell-specific deletion of the BK were subjected to the open-chest model of MI. Infarct sizes of the conditional mutants were compared to litter-matched controls as well as to global BK knockout (BK-KO) and wildtype mice. Cardiac damage was assessed after mechanical conditioning or pharmacological stimulation of the cGMP pathway and by using direct modulators of BK. Long-term outcome was studied with respect to heart functions and cardiac fibrosis in a chronic MI model.

**Results**—Global BK-KOs as well as CMBK-KOs, in contrast to SMBK-KOs, exhibited significantly larger infarct sizes as compared to their respective controls. Ablation of CMBK resulted in higher serum levels of cardiac troponin I as well as elevated amounts of reactive oxygen species, lower p-ERK/p-AKT levels and an increase in myocardial apoptosis. Moreover, CMBK was required to allow beneficial effects of both NO-GC activation and inhibition of the cGMP-degrading phosphodiesterase-5 (PDE5) as well as ischemic pre- (iPre) and postconditioning (iPost) regimens. To this end, after 4 weeks of reperfusion fibrotic tissue increased and myocardial strain echocardiography was significantly compromised in CMBK-deficient mice.

**Conclusions**—Lack of CMBK channels renders the heart more susceptible to I/R injury, whereas the pathologic events elicited by I/R do not involve BK in SM. BK seems to permit the protective effects triggered by cinaciguat, riociguat and different PDE5 inhibitors as well as beneficial actions of iPre and iPost by a mechanism stemming primarily from CMs. In summary, this study establishes mitochondrial CMBK channels as a promising target for limiting acute cardiac damage as well as adverse long-term events that occur after MI.

**Key Words:** infarct size; mitochondria; mouse mutant; cyclic nucleotide; potassium channels; Nitric oxide-sensitive guanylyl cyclase, voltage and  $\text{Ca}^{2+}$ -activated potassium channel BK, ischemic preconditioning, ischemic postconditioning, cardiomyocyte

## Clinical Perspective

### What is new?

- CMBK channel deficiency renders the heart highly vulnerable to ischemia and reperfusion injury.
- Beneficial effects of cardioprotective agents that are known to target the NO-GC/cGMP pathway require CMBKs.
- Ischemic pre- and post-conditioning procedures against I/R injury signal via CM-specific BK channels.
- cGMP/cGKI increase the open probability of BK channels in isolated inner membrane patches derived from CM mitochondria.
- Lack of CMBKs is associated with compromised post-MI heart function and accelerated fibrous tissue deposition.
- Under physiological conditions CMBK channels modulate contractile and chronotropic properties of the heart.



### What are the clinical implications?

- Activation of CMBK may represent a supportive strategy for limiting the cardiac damage during reperfusion therapy in acute myocardial infarction (AMI).
- By affecting cardiac contractility and infarct scar formation CMBK seems to be important for long-term outcome after AMI.
- Collectively, the *in vivo* data obtained should guide future clinical trials using either approved or new drugs to target a CM-specific NO-GC/cGMP/BK pathway in ischemic heart disease and its complications.

Myocardial infarction (MI) is one of the leading causes of death worldwide.<sup>1</sup> In addition to the acute damage, chronic heart failure may develop post-MI often severely limiting the patient's life. Hence, novel strategies and ideas to improve the outcome after MI are highly desired. Concepts aiming to reduce cardiomyocyte (CM) cell death during MI seem promising because the death of CMs represents a main cause of morbidity and mortality. Cell death during MI develops in response to the ischemic injury and in addition to reperfusion injury, which refers to the tissue damage caused when blood supply through the vessel is restored.<sup>2-4</sup> Reperfusion injury contributes to up to 50% of the final infarct size although fast re-opening of the occluded vessel is currently our best clinical therapy available for patients with MI.<sup>5</sup> Mechanical conditioning induced by short repetitive episodes of ischemia either before (iPre)<sup>6-10</sup> or directly after the ischemic period (iPost)<sup>11, 12</sup> proved an efficient method to reduce cell death, infarct size and thereby improve outcome in various animal models of MI; however, human trials have not translated these findings into clinical practice<sup>13-21</sup>.

Reportedly, activation of the nitric oxide-sensitive guanylyl cyclase (NO-GC) pathway signaling via cyclic guanosine-3',5'-monophosphate (cGMP) and cGMP-dependent protein kinase type I (cGKI) exhibited substantial protection against cardiac ischemia and reperfusion (I/R) injury<sup>8, 11, 22, 23</sup>. For example, administration of the NO-GC activator cinaciguat<sup>11, 23</sup> and the stimulator riociguat<sup>22</sup> as well as inhibition of cGMP-degrading PDEs i.e. PDE5 by using either sildenafil<sup>11, 24-26</sup>, vardenafil<sup>27</sup> or tadalafil<sup>28</sup> showed beneficial effects in various models of I/R injury and MI. The pharmacological conditioning-like signaling events downstream of cGMP during I/R need, however, further clarification. It was proposed that cGMP/cGKI in CMs and in isolated CM mitochondria cause an opening of mitochondrial ATP-dependent potassium channels (mitoK<sub>ATP</sub>)<sup>29</sup>, which have been shown to prevent the damaging effects of I/R in the

heart upon activation<sup>24, 30-32</sup>. These findings attracted our interest because they suggest that cGMP may be an upstream component of a cardioprotective pathway that involves potassium channels in the inner mitochondrial membrane. In addition to mitoK<sub>ATP</sub> potassium channels, several groups, including us, have reported evidence for Ca<sup>2+</sup>-activated K<sup>+</sup> channels of the BK type (BK) in CM<sup>33, 34</sup>. The pore-forming  $\alpha$ -subunit of BK is encoded by a single gene (*KCNMA1*, *SLO-1*) and usually located at the plasma membrane of cells; however, in CMs, BK is exclusively present in the inner mitochondrial membrane (IMM).<sup>33, 34</sup> By studying hearts obtained from mice with a global deletion of the BK channel (BK-KO) in an *ex vivo* Langendorff perfusion setup, we and others have confirmed that mechanical conditioning acts in favor of the myocardial survival by a BK-dependent effect on I/R<sup>12, 35, 36</sup> via limiting accumulation of excessive reactive oxygen species (ROS).<sup>34</sup> A burst of ROS occurring within the first minutes of reperfusion, when oxygen is re-introduced, seems to be a critical step for initiating a chain of detrimental events eventually leading to mitochondrial dysfunction and CM death.<sup>37</sup> Moreover, BK channel openers like NS1619 and NS11021 have been shown to prevent cardiac damage when applied before ischemia and at the early onset of reperfusion in different *ex vivo* settings.<sup>33, 38, 39</sup> However, one report did not find evidence for an altered response of the myocardium to the protection afforded by volatile anesthetics in the absence of BK.<sup>40</sup>

Because canonical BK channels are directly stimulated by cGMP/cGKI<sup>41-43</sup> we hypothesized that the cardioprotection afforded by cGMP-elevating compounds may also require CMBK activity in order to prevent cell death during I/R *in vivo*. To study this, here we applied an open chest *in situ* mouse model of MI and assessed infarct size in global BK-KO as well as in conditional BK mutants with a cardiomyocyte- or a smooth muscle cell-specific deletion of the BK channel (CMBK-KO or SMBK-KO, respectively) and compared the outcome to their litter-

matched controls. To validate the role of endogenous CMBK channels for the usually cardioprotective NO-GC/cGMP/cGKI pathway, we further studied the effect of cGMP-elevating compounds over the course of the myocardial I/R injury in our gene-targeted BK models. To this end, we identified endogenous CMBK channels as infarct limiting factors. Opening of CMBK channels measured by patch-clamp method in *ex vivo* mitoplast preparations occurs in a cGMP/cGKI-dependent mode and seems to be essential in order to establish cardioprotection elicited either by mechanical pre- and postconditioning procedures or by pharmacological cGMP-elevation *in vivo*.

## Methods

The data, analytic methods and gene-targeted mouse models used will be made available to other researchers for purposes of reproducing the results or replicating the procedure. Further information in this regard will be made available by contacting the corresponding author.

## Animals

All animal experiments were performed with permission of the local authorities and conducted in accordance with the German legislation on the protection of animals. Mice were kept in cages with wooden-chip bedding on a standard 12-hour light/dark cycle with ad libitum access to food and water under temperature and humidity control. Global BK channel deficient mice (*genotype*: BK<sup>-/-</sup>) and their wild-type littermates (*genotype*: BK<sup>+/+</sup>) on a mixed SV129/C57BL background were bred and maintained by at the Institute of Pharmacy, Department of Pharmacology, Toxicology and Clinical Pharmacy, University of Tuebingen as described before.<sup>44</sup>

By crossing transgenic mice that carry a Cre recombinase transgene under control of the myosin heavy chain 6c ( $\alpha$ MHC) promoter (*genotype*:  $\alpha$ MHC-Cre<sup>Tg/+</sup>) (Jackson Laboratory,



Stock No.: 011038)<sup>45</sup> to mice heterozygous for the BK gene locus (*genotype*: BK<sup>-/+</sup>) we produced a parental generation of  $\alpha$ MHC-Cre<sup>Tg/+</sup>; BK<sup>-/+</sup> mice for subsequent breeding steps. In order to generate experimental subjects with a CM-specific deletion of endogenous BK channels,  $\alpha$ MHC-Cre<sup>Tg/+</sup>; BK<sup>-/+</sup> mice were mated to our widely introduced floxed BK (BK<sup>fl/fl</sup>) mouse line allowing conditional loss-of-function studies *in vivo*.<sup>46-48</sup> From these crossings we established the CMBK-KOs (*genotype*:  $\alpha$ MHC-Cre<sup>Tg/+</sup>; BK<sup>-/fl</sup> or CMBK<sup>-/fl</sup>) and respective control mice from the same litters CMBK-CTR (*genotype*:  $\alpha$ MHC-Cre<sup>Tg/+</sup>; BK<sup>+/fl</sup> or CMBK<sup>+/fl</sup>). By an analogous approach we generated smooth muscle cell-specific BK mice (SMBK-KO; *genotype*: SMMHC-CreERT2<sup>Tg/+</sup>; BK<sup>-/fl</sup> or SMBK<sup>-/fl</sup>) and their respective controls (SMBK-CTR; *genotype*: SMMHC-CreERT2<sup>Tg/+</sup>; BK<sup>+/fl</sup> or SMBK<sup>+/fl</sup>) with SMMHC-CreERT2<sup>Tg/+</sup> representing a tamoxifen-inducible Cre recombinase under the control of the alpha myosin heavy chain 11 promoter<sup>49</sup>. With regards to the floxed BK gene loci the SMBK-KO mice remained pre-mutant until Cre activation by tamoxifen (1 mg/d, *i.p.*) for 5 consecutive days. After seven days or later after the last tamoxifen administration SMBK-KO and tamoxifen-injected SMBK-CTRs were used for the acute or chronic I/R experiments.<sup>46</sup> To study the infarct sizes in the acute I/R model (Suppl. Fig. 1), data from global and conditional BK male and female mice were combined as the amount of infarction did not differ between sex (Suppl. Fig. 2). For the SMBK mouse study only male subjects could be analyzed for their response to the cardiac I/R injury because the CreERT2-transgene was located on the Y-chromosome. All animals were investigated at an age of 8-16 weeks without observing age-related differences (Suppl. Fig. 3).

The specificity and efficiency of recombination in the  $\alpha$ MHC-Cre transgenic model was assessed after crossing these mice to double fluorescent ROSA26-tomato reporter animals (*genotype*: ROSA<sup>mTG/+</sup>)<sup>50</sup> obtained from Charles River (Jackson Laboratory, Stock No.: 007576).

The genotypes of the different mouse strains as well as the Cre-mediated somatic recombination events in cardiomyocytes and representative organs were determined by PCR amplification after DNA extraction using primer pairs that specifically identify the wildtype (+), knock-out (-) and floxed (fl) BK gene loci as previously described.<sup>44, 45, 49, 50</sup>

### Statistical analysis

All data are presented as means  $\pm$  SEM. Gaussian distribution was confirmed by Shapiro-Wilk test. The equality of group variances was tested using Levene's test. Statistical analysis was performed on experimental data consisting of two groups using either an unpaired Student's t-test for normally distributed data or Mann-Whitney-U test as non-parametric test. Comparison of more than two groups was evaluated using two-way analysis of variance (ANOVA) followed by unpaired Student's t tests with the Bonferroni correction for multiple comparison. For non-Gaussian distributed variables (> 2 experimental groups) a Kruskal-Wallis test followed by Dunn's test for multiple pairwise comparisons was performed. If Levene's test confirmed unequal variance, groups were compared by Welch's t-test. Mean arterial blood pressure measurement data were analyzed by repeated measures ANOVA followed by Bonferroni post-hoc test. For patch-clamp experiments one-way ANOVA was used to compare means of three or more treatment conditions within a genotype. If not otherwise indicated, differences between genotypes or groups were not significant. For all tests, a p-value less than 0.05 was considered as significant (\*/ $\dagger$   $p < 0.05$ , \*\*/ $\S$   $p < 0.01$ , \*\*\*/ $\#$   $p < 0.001$ ). Statistical analysis was performed using IBM SPSS statistic version 24.

See the online-only Data Supplement for a detailed description of the methods.



## Results

### Infarct sizes are increased in mice globally lacking BK channels

We studied the vulnerability of global BK-KO (BK<sup>-/-</sup>) mice against ischemia/reperfusion (I/R) injury in an *in vivo* model of MI. After 30 min ischemia followed by 120 min reperfusion (Suppl. Fig. 1, ①), area at risk (AAR in % of total heart area) neither differed across global BK-KO and litter-matched wild-type (BK-WT, BK<sup>+/+</sup>) groups nor between different experimental setups (Fig. 1A, Suppl. Fig. 1). Cardiac damage was not observed in sham operated subjects of both genotypes (Fig. 1B, middle, Suppl. Fig. 1, ②) supporting the high specificity and reproducibility of our *in vivo* I/R approach. Infarct size (as % of AAR) after I/R *per se* was significantly greater in BK-KO ( $38.56 \pm 1.65\%$  (n=11)) as compared to BK-WT ( $22.39 \pm 1.32\%$  (n=8), Fig. 1B, left) mice, suggesting an important role for BK channels for cardiac cell survival regardless of gender or age of the experimental animals (Suppl. Fig. 2+3). To confirm the histological results we measured cardiac troponin I (cTnI) levels in blood serum as an independent biomarker of cardiac cell death due to MI. Levels of cTnI increased immediately after I/R in both genotypes, but again mice with a global ablation of the BK channel exhibited significantly higher cTnI values as compared to BK-WT mice ( $7.78 \pm 1.48$  ng/ml for BK<sup>+/+</sup> (n=11),  $20.47 \pm 4.23$  ng/ml for BK<sup>-/-</sup> (n=8), Fig. 1C). In the isolated and perfused heart model we have previously observed that iPre requires BK channels in order to afford cardioprotection.<sup>34</sup> We now extended this finding to an established iPost procedure (Suppl. Fig. 1, ③) and found that cardiac damage was prevented in a BK-dependent mode ( $11.41 \pm 0.89\%$  for BK<sup>+/+</sup> (n=8),  $34.13 \pm 1.29\%$  for BK<sup>-/-</sup> (n=9), Fig. 1B, right). In support of recent studies that implicated BK-dependent protection against I/R-induced cell death was stemming from the CM itself, we first investigated the response to hypoxia of adult CMs obtained from global BK-KO hearts. Effects of oxygen-deprivation were evaluated by

light microscopy and by lactate dehydrogenase (LDH) release. In comparison to BK-WT CMs the data showed a clear tendency towards more cell death (Fig. 1D+E); however, this difference in LDH release did not reach the level of statistical significance.

### **CM-specific BK channel deficiency results in impaired heart functions *in vivo***

To clarify the cellular mechanisms whereby BK channels afford protection against I/R injury and in iPost signaling, we first generated gene-targeted mice lacking BK in CMs. In a first series of experiments, we assessed the recombination efficacy and specificity of the CM-restricted Cre recombinase<sup>45</sup> using a two-color fluorescent reporter system.<sup>50</sup> In the absence of  $\alpha$ MHC-Cre activity we observed ubiquitous expression of the cell membrane-targeted red fluorescent Tomato (mT) protein in the heart and aorta, with the latter being used as control tissue (Fig. 2A, Suppl. Fig. 4, left column). As expected,  $\alpha$ MHC-Cre-mediated excision of the loxP-flanked mT DNA sequence resulted in an almost complete switch (98.97%) to green fluorescent protein (mG) in cardiomyocytes (Fig. 2A right panels and 2B), whereas non-CMs such as coronary and aortic smooth muscle cells continued to express the mT protein (Suppl. Fig. 4 right column). Next, we applied a BK-specific primer set designed to identify the three different BK alleles *i.e.* wild-type (+), floxed (fl) and knockout (-) within one sample of different tissues derived from  $\alpha$ MHC<sup>Tg/+</sup>; BK<sup>+/fl</sup> mice. In line with the Cre-reporter study (Fig. 2A+B and Suppl. Fig. 4), the BK-specific PCR products confirmed efficient recombination of the endogenous BK gene locus in atrial and ventricular CMs (Fig. 2C). In contrast, conversion of the floxed BK allele was not observed in DNA purified from skeletal muscle, white adipose tissue (Fig. 2C), brain, liver or aorta (data not shown). In line with the conversion of the floxed BK DNA sequence to the respective (-) allele in CMs (Fig. 2C), immunoblots utilizing two different BK antibodies revealed a substantial decrease in BK channel protein levels from CMBK-KO mitochondria

purified from CMs (Fig. 2D+E). CMBK mutant mice did not develop any obvious phenotype and exhibit normal body and heart weights (Suppl. Tab. 1). Echocardiography, however, uncovered a mild reduction in the cardiac ejection fraction (%EF,  $64.63 \pm 1.83$  for CMBK<sup>+fl</sup> (n=8),  $58.97 \pm 1.56$  for CMBK<sup>-fl</sup> (n=9)), lower values for fractional shortening (%FS,  $35.14 \pm 1.38$  for CMBK<sup>+fl</sup>,  $30.99 \pm 1.07$  for CMBK<sup>-fl</sup>) and heart rate (HR,  $616 \pm 7$  for CMBK<sup>+fl</sup>,  $594 \pm 5$  for CMBK<sup>-fl</sup>) in the absence of CM BK channels (Fig. 3A-C). To investigate whether these differences in cardiac functionality were related to changes in hemodynamic parameters, telemetric blood pressure (BP) recordings were performed. Mean arterial pressure (MAP, Fig. 3D) was reduced in CMBK-KO mice ( $100.93 \pm 1.33$  mmHg (n=10)) as compared to litter-matched CMBK-CTRs ( $108.21 \pm 2.62$  mmHg (n=7)) with no effect on pulse pressure (Fig. 3E) or activity (data not shown). Lower MAP was related to an effect on systolic and diastolic values, but only for the latter this difference reached the significance level ( $p < 0.001$ ; data not shown).

### **CM-specific BK-KOs show a high susceptibility to the I/R damage**

As observed in the global BK-KO mice, I/R vulnerability of CM-specific BK channel mutants was higher as compared to the respective control mice ( $38.26 \pm 1.55\%$  for CMBK<sup>-fl</sup>,  $27.19 \pm 1.25\%$  for CMBK<sup>+fl</sup> (n=8 each), Fig. 4B left) with no apparent age or gender differences (Suppl. Fig. 2+3), whereas AAR among genotypes were similar irrespective of the experimental procedure (Fig. 4A, Suppl. Fig. 5A-C), and sham treatments did not evoke any significant cardiac damage (Fig. 4B right). Consistent with the histological data, cTnI levels in the blood serum measured directly after I/R procedure were significantly elevated in CMBK-KO mice ( $7.34 \pm 1.82$  ng/ml for CMBK<sup>+fl</sup> versus  $20.06 \pm 3.45$  ng/ml for CMBK<sup>-fl</sup> (n=8 each), Fig. 4C). To verify that the higher vulnerability of the CMBK-KO hearts to the I/R stimulus was not due

to an unexpected hemodynamic response under anesthesia, BP was measured in unconscious mice. Anesthesia induced by pentobarbital- $\text{Na}^+$  injection resulted in a comparable decrease in the MAP of CMBK-CTR and CMBK-KO mice (Suppl. Fig. 6A) suggesting that the differences in infarct size between both genotypes were unrelated to the hypotension observed after CMBK channel ablation (Fig. 3D). Moreover, we measured coronary flow (CF) during reperfusion after 30 min ischemia in isolated Langendorff-perfused CMBK-KO and -CTR hearts with no apparent differences between genotypes (Suppl. Fig. 6B+C). To further exclude the possibility that vascular BK channels affect the cardiac I/R phenotype, we subjected gene-targeted mice carrying a smooth muscle cell-specific ablation of the BK channel (SMBK-KO,  $\text{SMBK}^{-/\text{fl}}$ )<sup>46</sup> to the I/R injury. After Cre-mediated conversion of the floxed BK locus specifically in smooth muscle cells (Suppl. Fig. 7A) tamoxifen-treated SMBK-KO and -CTR mice were examined for their response to the I/R procedure and iPost. SMBK-KO mice, in contrast to the CMBK-deficient mutants, exhibited infarct sizes that were similar to their respective litter-matched controls and AARs that did not differ between SMBK-deficient and proficient mice (Suppl. Fig. 7B+C). Together, the findings from different gene-targeted mouse models support the notion that CMBK but not SMBK channels are key elements of a cardioprotective pathway.

### **CMBK ablation affects ROS formation, apoptosis and the reperfusion injury salvage kinase pathway at I/R**

We and others have previously presented *in vitro* evidence for a link between BK channels exclusively localized at the inner mitochondrial membrane of the CMs and ROS dynamics during hypoxia.<sup>34</sup> Because ROS is a major determinant of the myocardial damage at I/R *in vivo* we herein investigated whether the enlarged infarct sizes in CMBK-KOs were due to an effect on the amount of cardiac ROS production. *In vivo* mitochondrial production of superoxide leading

to hydrogen peroxide formation can be estimated by defining the ratio of MitoP to MitoB after a single MitoB bolus.<sup>51</sup> At baseline we observed a mildly reduced MitoP/MitoB ratio in CMBK-KOs, which was elevated after I/R (Suppl. Fig. 8A). Normalization of the values demonstrated a significant higher increase in hydrogen peroxide formation in I/R-exposed CMBK-deficient hearts (Fig. 4D), an effect that was unrelated to the expression of ROS degrading enzymes such as CuZnSOD (SOD1) and MnSOD (SOD2) (Suppl. Fig. 8B-D). Furthermore, at normoxia mitochondria from BK-proficient and -deficient CMs displayed no defects in any of the bioenergetics variables studied (Suppl. Fig. 9A-C). Cell death by apoptotic mechanisms represents a further indicator of outcome after MI.<sup>52</sup> Apoptosis was determined by DNA strand breaks using the TUNEL method on eight equidistant regions between the cardiac apex and the ligation (Fig. 4E). Overall, the number of TUNEL-positive cells in CMBK mutant hearts ( $3.99 \pm 0.81\%$ ) was higher as compared to CMBK-CTR hearts ( $2.64 \pm 0.52\%$  ( $n=3$  per genotype), Fig. 4F) after I/R. In a central area covering heart regions 2-4, which relate to a pronounced part of the infarct according to the TTC staining, apoptosis rates between genotypes were significantly different with higher values for CMBK-KO hearts (Fig. 4G). Apparently, CMBK activity affects both forms of cell death that occur simultaneously during MI. Activation of the pro-survival kinases of the reperfusion injury salvage kinase (RISK) pathway ERK and Akt<sup>53,54</sup> was assessed using phospho-specific antibodies. After I/R with 10 min reperfusion (I/R<sub>10</sub>) p-ERK/ERK and p-Akt/Akt ratios showed a small but significant increase in CMBK-CTR heart lysates, which was less pronounced in the absence of CMBK channels (Fig. 4 H+I).

### Mechanical conditioning procedures, pharmacological conditioning by cGMP-elevating compounds and direct activators of BK protect the heart via BK channels in CMs

As expected, mechanical conditioning either by iPost or by iPre procedures (Suppl. Fig. 1, ③+④) efficiently protected CMBK-CTR hearts from I/R damage (*iPost* infarct size:  $11.27 \pm 0.62\%$ , *iPre* infarct size:  $13.13 \pm 1.05\%$ ). The beneficial effects of both mechanical interventions were largely attenuated in CMBK-KO mice (*iPost* infarct size:  $28.26 \pm 1.52\%$ , *iPre* infarct size:  $28.77 \pm 0.58\%$  (n=8 per genotype and setup), Fig. 5A). A direct comparison of infarct size at iPost (in % to I/R without stimulus) between CMBK positive and negative hearts revealed that CM-specific BK channels account for >50% of the protection afforded by iPost (Fig. 5B, left). In comparison to CMBK-KO hearts, the beneficial effects of the iPost procedure on global BK-KO hearts were lower (Fig. 5B, right) suggesting either remaining traces of CMBK channel activity in the Cre-based model (see also Fig. 2D+E) or non-CMs BK channels as additional mediators of the signaling elicited by iPost. In order to test whether the acute targeting of the BK resembles the cardiac I/R damage observed in the gene-targeted models we used paxilline an established BK blocker (Suppl. Fig. 1, ⑤). With paxilline infarct size in CMBK-CTR mice ( $35.9 \pm 6.2\%$  (n=8)) increased to the levels seen in the respective CMBK-KOs ( $36.97 \pm 1.69\%$ , n=8) (Fig. 5C, left). Importantly, paxilline had no significant effect on the I/R damage that develops in response to I/R in CMBK-deficient hearts (compare Fig. 4B with 5C, left and Fig. 5D, left). Conversely, we used the BK channel opener NS11021 to test for cardioprotective effects of CMBK activation (Suppl. Fig. 1, ⑥). A significant reduction in infarct size by  $44.7 \pm 5.6\%$  was observed when NS11021 (9.2  $\mu\text{g}$  per kg) was administered to CMBK-CTR mice prior to the reperfusion (NS11021 infarct size:  $15.05 \pm 1.52\%$  (n=8), Fig. 5C+D, right), whereas the protection elicited by NS11021 was significantly lower in CMBK-KO hearts (NS11021 infarct size:  $32.66 \pm 0.82\%$

(n=8), Fig. 5C, right). With 9.2  $\mu\text{g}$  per kg NS11021 we did not observe any toxic side-effects; however, with higher dosage of the compound (i.e. 92  $\mu\text{g}$  per kg) we observed that 37.5% of the experimental mice died during reperfusion irrespective of their genotype. Control experiments performed using the solvents used for paxilline or NS11021 showed that the solvents did not affect infarct size formation at I/R conditions (Suppl. Fig. 5D).

Because canonical BK channels usually present at the plasma membrane of various cell types are directly phosphorylated by cGMP/cGKI<sup>43</sup>, we studied whether the infarct limiting effects of pharmacological modulators that stimulate the NO-GC/cGMP/cGKI pathway involve CMBK channels.

Importantly, neither the cardiac expression of cGKI nor its enzyme activity, which was monitored by assessing the phosphorylation of the Ser239 residue in the vasodilator-stimulated phosphoprotein (VASP), was affected by the lack of CMBK channels (Suppl. Fig. 10). I/R<sub>10</sub> resulted in a mild increase in pVASP level, but no apparent differences between both genotypes. Most noteworthy, in the presence of CMBK, both the NO-GC stimulator riociguat (Suppl. Fig. 1, 7) as well as the heme-independent NO-GC activator cinaciguat (Suppl. Fig. 1, 8) reduced the infarct area by  $42.5 \pm 9.6\%$  (*RIO* infarct size:  $15.63 \pm 2.60\%$  (n=8), Fig. 6A+B, left) and by  $50.5 \pm 4.7\%$  (*CIN* infarct size:  $13.46 \pm 1.28\%$  (n=8), Fig. 6A+B, right), respectively. A direct comparison of the infarct sizes in the riociguat and cinaciguat groups to the I/R condition showed that the cardioprotection afforded by riociguat was strongly attenuated (*RIO* infarct size:  $31.28 \pm 2.62\%$  (n=10)) or completely abolished for the cinaciguat treatment (*CIN* infarct size:  $38.20 \pm 1.69\%$  (n=8)) in CMBK-KO mice suggesting that cardioprotection via NO-GC/cGMP requires functional CMBK. Using a FRET-based cGMP sensor we confirmed a small but continuous increase in CM-specific cGMP after cinaciguat administration *in situ* (Suppl. Fig. 11).

Accordingly, the inhibition of cGMP-hydrolyzing PDEs by sildenafil and tadalafil (Suppl. Fig. 1, 9 and 10) reduced the cardiac I/R injury in CMBK-CTR (*SIL* infarct size:  $11.64 \pm 0.91\%$  (n=8), *TAD* infarct size:  $14.38 \pm 1.15\%$  (n=9)) but not in CMBK-KO (*SIL* infarct size:  $35.59 \pm 1.51\%$  (n=8), *TAD* infarct size:  $32.47 \pm 2.43\%$  (n=9), Fig. 6C+D) or global BK-KO mice (Suppl. Fig. 12). Again, the respective solvents did not influence the amount of infarction (Suppl. Fig. 5E). As the cardioprotective effects of iPost and sildenafil were abolished by L-NAME co-treatment (Fig. 6E+F), we conclude that endogenous NO signaling is involved in the CMBK-dependent modulation of cardiac damage. In addition, L-NAME, which was given over 4-5 days prior to the I/R procedures (Suppl. Fig. 1, 11), affected various hemodynamic parameters of the mice via a CMBK-independent mechanism (Suppl. Fig. 13A+B) whereas the inhibition of NO synthesis *per se* did not modulate infarct sizes after I/R (compare Fig. 4B with Suppl. Fig. 13C).

### **Mitochondrial BK channels in isolated membrane patches are directly activated by cGMP/cGKI**

In our quest to understand how cGMP and mitochondrial BK channels in CMs are connected at a molecular level, we made use of two different antibodies specifically recognizing common regions in the major cardiovascular cGMP effector protein cGKI. By studying total heart lysates and purified mitochondrial protein fractions derived from BK-deficient and -proficient CM mitochondria we demonstrated that cGKI is present in the lysates as well as in the mitochondrial protein fraction, whereas cytosolic or plasma membrane bound proteins such as  $\alpha$ -tubulin- or  $\beta_1$ -adrenoreceptor were not observed in the mitochondrial protein fraction, respectively (Fig. 7A and Suppl. Fig. 14A-C). To test if cGMP/cGKI directly modulates mitochondrial BK activity, we performed patch-clamp experiments on isolated mitoplast membrane patches obtained from CM mitochondria by osmotic swelling (Suppl. Fig. 15). Previously, three active mitoplast channels of



370 pS, 120 pS and 60 pS as well as a BK-specific channel activity of 190 pS were detected in whole mitoplasts derived from BK-proficient CMs.<sup>34</sup> All but the latter conductance were observed in BK-deficient mitoplasts. In the present patch-clamp approach using inner mitochondrial membranes (IMM) we detect all of the previously identified channel conductances; however, due to differences in ionic composition the corresponding conductance activities were 345 pS (not shown), 145 pS, 95 pS and 35 pS (not shown) (s. Fig. 7). Importantly, and in a good agreement with our previous report the 145 pS conductance was detected in 65% IMM patches from BK-WT (n=70) but not in BK-KO mitoplasts (n=33). Besides a slightly smaller conductance this channel displayed a linear current-voltage relationship (Fig. 7B) and several other characteristics of the canonical BK channel usually present at the plasma membrane of cells (Fig 7C-D). As reported previously,<sup>34</sup> the mitochondrial BK opened with rare bursts with short closed dwell times at negative voltages and at positive voltages with longer and more frequent openings (Fig 7C). Moreover, the open probability ( $P_o$ ) of the channel was sensitive to  $Ca^{2+}$  (Fig 7D, left panel), stimulated by NS11021 and inhibited by paxilline (Fig 7D, right panel), which allowed us to assign the 145 pS activity with high confidence to the mitochondrial BK channel. Importantly, a prevailing conductance of rather similar appearance (95 pS) was present in BK-WT and BK-KO IMM patches suggesting it constitutes a channel different from BK (Fig. 7F). To investigate whether cGMP/cGKI modulates the mitochondrial BK channel we measured IMM patches displaying BK in the presence of  $Mg^{2+}$ /ATP, the cGMP analog 8-Br-cGMP and cGKI (Fig 7E+F). Consistent with previous observations the presence of  $Mg^{2+}$ /ATP caused a significantly lower  $P_o$  of the mitochondrial BK.<sup>55</sup> Subsequent addition of cGMP and cGKI to the same patches dramatically increased the  $P_o$  as a strong indicator for the positive regulation of mitochondrial BK occurring due to the 8-Br-cGMP/cGKI-dependent

phosphorylation of the channel. Importantly, this stimulated channel activity was sensitive to paxilline and was found very frequently in mitoplasts derived from BK-WT CMs (n=7), whereas neither the 95 pS channel activity (n=5) nor the 345 pS channel activity (data not shown) in BK-KO mitoplasts was modulated by cGMP/cGKI (Fig. 7F). Collectively, these electrophysiological experiments on IMM patches establish an evidence for a molecular connection between cGMP/cGKI and BK channel function at the IMM.

### **Lack of CMBK channels aggravates cardiac dysfunctions post-MI**

So far our data support the notion that CMBK channels prevent acute I/R injury. To test for a potential role of BK for the long term outcome after I/R, we investigated a chronic mouse model of MI with 30 min ischemia followed by 4 weeks reperfusion (I/R<sub>4wks</sub>). Interestingly, overall survival of the CMBK-KO and -CTR mice as well as their post-MI heart weights (Suppl. Tab. 2) were not different. Longitudinal strain, which characterizes the endocardial shortening of the myocardial fibers during systole (Fig. 8A, diastole=0), represents one of the earliest and most sensitive markers of cardiac dysfunction.<sup>56, 57</sup> We assessed the synchronicity of the longitudinal strain by echocardiography in six endocardial segments during systole and diastole in CMBK-KO mice and observed mild alteration under basal conditions (Suppl. Fig. 16A+B) and a heavily disturbed synchronicity after I/R<sub>4wks</sub> (Suppl. Fig. 16C+D). In particular in the anterior apex (AA) region myocardial deformation was dramatically altered in the absence of CMBK. Quantification of the longitudinal strain (Fig. 8A) over all segments confirmed abnormal myocardial tissue deformation for CMBK-KO ( $-9.77 \pm 0.76\%$ ) as compared to litter-matched control hearts ( $-12.38 \pm 0.97\%$  (n=13 per genotype), Fig. 8B) and for both genotypes a significantly impaired deformation post-MI in comparison to basal levels ( $p < 0.001$ , Fig. 8B and Suppl. Fig. 16E). Additional parameters such as the radial strain and the strain rate exhibited only minor changes

between CMBK-KO and CMBK-CTR mice after I/R<sub>4wks</sub> (data not shown). Post-MI global ejection fraction was just not different between genotypes (Fig. 8C and Suppl. Fig. 16F) although by this time we observed a substantial increase in the amount of fibrosis as a pathological marker of the remodeling in CMBK-deficient hearts ( $15.63 \pm 1.40\%$  for CMBK<sup>+/-</sup>,  $22.49 \pm 1.89\%$  for CMBK<sup>-/-</sup> (n=13 per genotype), Fig. 8D). Differences between genotypes were further highlighted by plotting the amount of cardiac fibrosis against the individual decline in EF at 28 days post-MI (Suppl. Fig. 16G). By stratifying the post-MI EF as a long term outcome (Fig. 8C) for the initial means of the infarct sizes (Fig. 4B) we found significantly lower values for the CMBK-KO group suggesting an abnormal relationship between structural and functional properties of the BK-negative myocardium (Suppl. Fig. 16H).



## Discussion

At the moment, the best clinical therapy for the management of an acute MI represents the fast re-opening of the occluded coronary artery. In addition to the ischemic episode during MI, reperfusion damage of previously viable tissue is a major cause of CM death.<sup>2</sup> Strategies to target reperfusion injury have been studied extensively but with little success in patients.<sup>21, 58</sup> The modulation of the NO-GC/cGMP/cGKI pathway has attracted increasing attention because a number of studies suggested its infarct limiting capacities.<sup>11, 22-26, 28</sup> However, little is known about the mechanisms and downstream targets of this cardioprotective pathway. In addition to mitochondrial K<sup>+</sup> channels of the K<sub>ATP</sub>-type, which reportedly oppose mitochondrial dysfunction, excessive ROS production and Ca<sup>2+</sup> overload and hence the opening of the mitochondrial permeability transition pore (mPTP)<sup>24, 29, 30, 32</sup>, we assessed whether BK channels present in CM mitochondria are needed to allow the cardioprotective signaling elicited by iPre,

iPost and cGMP-elevation in an *in vivo* model of I/R.<sup>31, 35, 36</sup> We studied I/R in mice with a global deletion of the BK channel as well as conditional mutants lacking the BK channel exclusively in CMs and compared the outcome to the corresponding litter-matched controls, or to gene-targeted mutants lacking BK in smooth muscle cells. Interestingly, infarct size was significantly increased in global BK-KO mice (Fig. 1B), indicating that functional BK channels are important modulators of the myocardial response to the I/R injury an effect that was seen independently of the presence or absence of any cardioprotective stimuli. In contrast, global BK-KO hearts did not show evidence for a higher I/R vulnerability *ex-vivo*<sup>34</sup> and infarct size *per se* was also not sensitive to the BK channel blocker paxilline applied to Langendorff-perfused wildtype-hearts.<sup>26</sup> Apparently, the integration of the heart at the whole animal level is important in order to permit anti-infarct effects via endogenous BK channels. Because these initial analyses of the global BK-KOs did not allow us to conclude that the protection afforded was due to the BK in the CM or other cardiac cell types we assessed the amount of ischemic myocardium after I/R injury in two conditional mouse mutant lines that lack the BK channel either in CMs or in smooth muscle cells. Indeed, CMBK-KOs (Fig. 4B), but not SMBK-KO mice (Suppl. Fig. 7C), subjected to the I/R injury exhibited cardiac damages that amounted to the levels seen in global BK-KOs (Fig 1B), a finding that was confirmed by the elevated cTnI levels in the serum of both global and CM-specific BK-KOs (Fig. 1C+4C). The significant increase in the I/R-induced apoptotic cell death of CMBK-negative hearts (Fig. 4G) further supports the notion that CMBKs are the major BK channel population to protect CMs against the detrimental events elicited by I/R, an effect that was not related to changes in coronary flow (Suppl. Fig. 6B+C). Our approaches modulating the activity of BK by pharmacological means are consistent with the I/R data from the tissue-specific BK mouse models. Accordingly, the BK blocker paxilline (Fig. 5C) or the BK opener

NS11021 (Fig. 5C) aggravated or limited the infarcts of CMBK proficient animals, respectively. By comparing these results to the response of the CMBK-deficient hearts to paxilline and NS11021, we recognized an inadequate level of CM-specific BK channel activity as a major determinant of I/R-induced cell death. NS11021 has previously been used with success in *ex vivo* studies to induce cardioprotection<sup>38,59</sup>, a finding that we extended to show the favorable impact of this compound on infarct size *in vivo* (Fig. 5C). In this regard, it is important to note that we also recognized a dose-dependent toxicity of NS11021 (data not shown). Yet, specific openers of this channel should be further investigated towards a potential improvement of cardioprotective therapies in patients with acute MI.

Mitochondrial ROS *i.e.* superoxide that leads to the formation of hydrogen peroxide, can exert contrasting effects on the cardiac muscle during I/R. For example, a burst of ROS occurring at the early onset of reperfusion triggers the opening of the mPTP, which induces the collapse of the mitochondrial membrane potential, leading to ATP-depletion and cell death<sup>60</sup>, whereas low amounts of ROS lead to cardioprotection.<sup>30</sup> In the *in vivo* I/R model the elevated myocardial damage observed in the CMBK-deficient hearts correlated with a small but significant higher ROS increase after I/R compared to normoxic levels (Fig. 4D). Because isolated mitochondria obtained from global BK-KO hearts produce a higher level of ROS after anoxia followed by reoxygenation,<sup>34</sup> we conclude that functional BK channels regulate ROS homeostasis in oxidatively stressed CM mitochondria. Obviously, additional evidence is needed in order to establish the link between excessive mitochondrial ROS amounts and the dynamics of the K<sup>+</sup> influx and efflux pathways (potentially involving e.g. Connexin 43) in the I/R-exposed inner mitochondrial membrane.<sup>61-65</sup> Interestingly, a high mitochondrial matrix K<sup>+</sup> content reportedly provoke a mild uncoupling of the ETC thereby leading to low amounts of ROS that

eventually activate PKC and the cardioprotective RISK pathway.<sup>30, 31</sup> In addition to the link between mitochondrial K<sup>+</sup> channels and ROS, BK activity may confer cardioprotection at reperfusion by opposing the Ca<sup>2+</sup> overload that mediates MPTP opening and maintaining the membrane potential.<sup>33, 35, 36, 66, 67</sup> The putative signaling mechanisms involving BK in the CM during I/R *in vivo* as well as mechanistic limitations of the present study are summarized in Suppl. Fig. 17A+B.

Pro-survival protein kinases of the RISK pathway represent important signaling elements that confer cardioprotection at I/R in mice and rats, however, their activation has also been studied in larger animals with inconsistent results.<sup>25, 68-70</sup> At the onset of reperfusion phosphorylation of ERK1/2 and Akt seems to limit mPTP opening and thereby myocardial infarct size through various downstream targets of the RISK pathway, which include GSK-3 $\beta$  and eNOS among others (Suppl. Fig. 17A+B).<sup>31, 54, 71</sup> Interestingly, p-ERK1/2 and p-Akt levels were less increased after I/R<sub>10</sub> in CM-specific BK-KO hearts (Fig. 4H) suggesting a proper recruitment of Akt- and ERK1/2-dependent pathways requires the opening of BK channels. The RISK pathway is activated in the setting of iPost and we demonstrate that mechanical conditioning by iPost (and iPre) involves CM-specific BK channels. About 50% of the protection elicited by iPost in control hearts was lost in the absence of CMBK (Fig. 5B). Residual protection by iPost in the CMBK-KO heart may be established through recruitment of K<sub>ATP</sub> channels. Indeed, a large body of work suggests that mitochondrial K<sub>ATP</sub> channel opening plays a role in cardioprotection elicited by ischemic and pharmacological preconditioning and by iPost.<sup>72</sup> Consistent with this concept, the infarct area in I/R-exposed hearts from mice globally lacking BK was approximately 10% smaller with iPost than due to the I/R injury per se (Fig. 5B). The differences in the response of the two gene-targeted BK mouse lines was expected because *i.*) yet

to be identified non-myocyte BK channels may also play at least a minor role for iPost to establish full cardioprotection and *ii.*) the depletion of the CM-specific BK protein in the conditional mouse model did not reach the level of the global BK-KOs (s. also Fig. 2D+E). The NO-GC/cGMP pathway has been intensively studied for its cardioprotective properties in mice and in other animal models of I/R injury. Mechanisms responsible for the protective actions *i.e.* the downstream effectors of the pathway remain to be fully elucidated. Independently a number of investigators observed that either pharmacological modulators of NO-GC<sup>11, 22, 23</sup> or inhibitors of cGMP-degrading PDEs<sup>11, 25, 28</sup> exert cardioprotection via cGKI in the CM.<sup>11</sup> In contrast to the high vulnerability of the CMBK-deficient myocardium, a loss of CM-specific cGKI activity *per se* did not render the heart more or less resistant to the I/R injury.<sup>11</sup> Apparently, the pathophysiological reaction of the cardiac muscle is modulated by mitochondrial BK channels, whereas the significance of the NO-GC/cGMP/cGKI pathway in controlling infarct formation is best seen in mechanical and pharmacological conditioning-like settings. With regards to a link between NO-GC/cGMP and BK in the I/R exposed myocardium our findings suggest that the opening of CM-specific BK channels is an essential step in establishing protection by cGMP and cGMP elevating compounds. For example, either the stimulation of NO-GC by riociguat at the onset of reperfusion or by applying a preconditioning-like protocol using the NO-GC activator cinaciguat produced powerful cardioprotection when functional CMBK channels were present (Fig. 6A). Because cinaciguat resulted in a CM-specific increase in cGMP levels we suggest that the cGMP cascade was indeed stimulated under these experimental conditions (Suppl. Fig. 11). In addition to the infarct-limiting effects of NO-GC/cGMP, cardioprotection induced by sildenafil seems to be through cardiac BK channel complexes. A knock-down of the accessory  $\beta_1$ -subunit of the BK channel prior to I/R or co-

administration of the BK channel blocker paxilline efficiently blocked the beneficial effects of sildenafil in the *ex vivo* Langendorff-perfused heart model.<sup>26,73</sup> In accordance with these studies we applied sildenafil at the onset of reperfusion (Fig. 6C+D) and at the concentration used its cardioprotective potential was only observed in BK-proficient mice. By adopting a previously published preconditioning-like protocol<sup>28</sup> we also used tadalafil as an alternative and more selective inhibitor of the cGMP-degrading PDE5. In agreement with the sildenafil treatment study, the favorable effects of tadalafil on infarct formation were abolished in the CMBK gene-targeted mutants (Fig. 6C+D). Collectively, these findings point to the recruitment of a CM-specific BK channel to a cardioprotective cGMP/PDE5 pathway following the I/R injury. Because the presence of PDE5 in the CMs is a matter of ongoing debate<sup>74</sup>, it is important to consider non-CMs such as endothelial cells, immune cells and/or fibroblasts as the primary target of sildenafil and tadalafil. Taking all these considerations into account we believe it is possible that PDE5 inhibition during cardiac I/R involves the transfer of a protective signal from the non-CMs to the CMs. Paracrine features that may orchestrate a CMBK-dependent pathway in CMs may involve *e.g.* the induction or suppression of cytokines and growth factors, the precise nature of the I/R triggered intercellular communication between the different cardiac cell types, however, is still elusive and awaits further investigation.<sup>75</sup>

Our combined pharmacological and genetic strategy did not clarify how NO-GC/cGMP interact with the CMBK channel *in vivo i.e.* it remains unclear whereby the cytoplasmic cGMP signal was conferred to a potassium channel at the inner mitochondrial membrane. In addition to other lines of evidence provided by this study, the presence of the cGKI protein in mitochondrial fractions obtained from CMs further suggests that the protective signal is transduced via the cGMP/cGKI pathway (Fig. 7A). A notion that is also supported by the electrophysiological



measurements that demonstrated a direct molecular connection between cGMP/cGKI and BK channel in purified IMM patches (Fig. 7E+F). Finally, our data also support the view that sildenafil, sildenafil-sensitive cGMP-PDEs as well as iPost act through a NO-GC-dependent cGMP pathway against cardiac damage as L-NAME abolished any favorable effect of sildenafil or iPost on infarct size (Fig. 6E).<sup>76</sup>

In contrast to global BK-KO mice, CMBK mutants exhibited low blood pressure under physiological conditions.<sup>77</sup> Mild hypotension was accompanied by a slight decreases in heart rate, fractional shortenings and ejection fractions (Fig. 3 and data not shown). Because renovascular, baro-receptor, and neuro-endocrine mechanisms that usually maintain blood pressure homeostasis should not be affected by the CM-specific ablation of the BK channel in CMBK mutant mice we suggest an intrinsic cardiac dysfunction as major cause for the blood pressure phenotype. Previously, we observed a reduction of oxidative phosphorylation (OXPHOS) capacity and thus a deficit in ATP-generation of isolated ventricular muscle fibers obtained from global BK-KO mice.<sup>34</sup> However, mitochondrial bioenergetics, at least as measured in cell-free CM mitochondria, seem to be intact (Suppl. Fig. 9), together suggesting a more complex cross-talk between BK channel function and ATP-generation in mitochondria with putative upstream elements on the cytoplasmic side of the CM or muscle fiber. To this end, we speculate that the impaired cellular energy production by the mitochondrial OXPHOS system *in vivo* is linked to an abnormal resting heart rate and cardiac malfunctions in the CMBK-KO mouse model.

Based on the findings from the acute model, we studied the long-term outcome of CMBK-KO mice subjected to a chronic *in vivo* model of myocardial infarction. Although we did not observe differences in heart weight or ejection fraction between mice lacking the CMBK and

their litter-matched controls after ischemia followed by 4 weeks reperfusion, longitudinal strain as an early and sensitive marker for cardiac dysfunction<sup>56, 57</sup> was significantly reduced in CMBK-KO (Fig. 8). This functional deterioration was related to an increase in fibrotic scar formation, indicating that the CMBK channels may turn out to be important classifiers for the long-term prognosis after MI, as well.

In summary, the presented data establish infarct-limiting effects for endogenous CM-specific BK channels during I/R injury. Lack of CMBK resulted in mitochondrial ROS overproduction, an increase in CM apoptosis, and an improper activation of the pro-survival kinases ERK1/2 and Akt (summarized in Suppl. Fig. 17). Our supporting long-term study also implied a role for CMBK in limiting post-MI cardiac dysfunctions due to the accumulation of fibrous tissue. Finally, cardioprotection elicited by mechanical methods which block coronary blood flow as well as pharmacological agents that stimulate the NO-GC/cGMP pathway collectively depended on the BK status of the CM and 8-Br-cGMP/cGKI activate BK channels present in IMM. Hence, the current work highlights CM-specific mitochondrial BK channels as a novel target in reperfusion therapy and cardiac remodeling occurring post-MI.

### **Acknowledgments**

The authors thank Isolde Breuning and Michael Glaser (both from the Department of Pharmacology, Toxicology and Clinical Pharmacy, Institute of Pharmacy, University of Tuebingen, Tuebingen, Germany) for excellent technical help.

## Sources of Funding

Work in our laboratories is supported by the Deutsche Forschungsgemeinschaft (DFG) with grants to RL and PR and by the DFG Research Unit 2060 “cGMP signaling in cell growth and survival” to RL. The DFG funded Klinische Forschergruppe (KFO274) contributed to parts of the study. SF received funding from the Boehringer Ingelheim Fonds and MPM from the Medical Research Council UK (MC\_U105663142) and by a Wellcome Trust Investigator award (110159/Z/15/Z).

## Author contributions

Research design: RL; conducted experiments: SF, PB, AK, NB, JS, PK, AW, EM, and AL; contributed new reagents, techniques or analytic tools: JS, AL, MG, TK, MPM, AS, and VON; data analysis: SF, PB, NB, AK, JS, AL, AS, VON, PR and RL; contributed to discussions: JS, TK, AS, VON and PR; edited the manuscript: TK, MPM and PR; wrote or contributed to the writing of the manuscript: SF, PB, AK, NB and RL; approved the final manuscript: all authors.

## Disclosures

On behalf of all authors, the corresponding author states that there is no conflict of interest.

## References

1. Writing Group M, Mozaffarian D, Benjamin EJ, Go AS, Arnett DK, Blaha MJ, Cushman M, Das SR, de Ferranti S, Despres JP, Fullerton HJ, Howard VJ, Huffman MD, Isasi CR, Jimenez MC, Judd SE, Kissela BM, Lichtman JH, Lisabeth LD, Liu S, Mackey RH, Magid DJ, McGuire DK, Mohler ER, 3rd, Moy CS, Muntner P, Mussolino ME, Nasir K, Neumar RW, Nichol G, Palaniappan L, Pandey DK, Reeves MJ, Rodriguez CJ, Rosamond W, Sorlie PD, Stein J, Towfighi A, Turan TN, Virani SS, Woo D, Yeh RW, Turner MB, American Heart Association Statistics C and Stroke Statistics S. Heart Disease and Stroke Statistics-2016 Update: A Report From the American Heart Association. *Circulation*. 2016;133:e38-360.

2. Garcia-Dorado D. Myocardial reperfusion injury: a new view. *Cardiovasc Res.* 2004;61:363-364.
3. Ibanez B, Heusch G, Ovize M and Van de Werf F. Evolving therapies for myocardial ischemia/reperfusion injury. *J Am Coll Cardiol.* 2015;65:1454-1471.
4. Heusch G and Gersh BJ. The pathophysiology of acute myocardial infarction and strategies of protection beyond reperfusion: a continual challenge. *Eur Heart J.* 2017;38:774-784.
5. Hausenloy DJ and Yellon DM. Myocardial ischemia-reperfusion injury: a neglected therapeutic target. *J Clin Invest.* 2013;123:92-100.
6. Guo Y, Wu WJ, Qiu Y, Tang XL, Yang Z and Bolli R. Demonstration of an early and a late phase of ischemic preconditioning in mice. *Am J Physiol.* 1998;275:H1375-1387.
7. Schwanke U, Konietzka I, Duschin A, Li X, Schulz R and Heusch G. No ischemic preconditioning in heterozygous connexin43-deficient mice. *Am J Physiol Heart Circ Physiol.* 2002;283:H1740-1742.
8. Sips PY, Brouckaert P and Ichinose F. The alpha1 isoform of soluble guanylate cyclase regulates cardiac contractility but is not required for ischemic preconditioning. *Basic Res Cardiol.* 2011;106:635-643.
9. Murry CE, Jennings RB and Reimer KA. Preconditioning with ischemia: a delay of lethal cell injury in ischemic myocardium. *Circulation.* 1986;74:1124-1136.
10. Hausenloy DJ, Barrabes JA, Botker HE, Davidson SM, Di Lisa F, Downey J, Engstrom T, Ferdinandy P, Carbrera-Fuentes HA, Heusch G, Ibanez B, Iliodromitis EK, Inzerillo J, Jennings R, Kalia N, Kharbanda R, Lecour S, Marber M, Miura T, Ovize M, Perez-Pinzon MA, Piper HM, Przyklenk K, Schmidt MR, Redington A, Ruiz-Meana M, Vilahur G, Vinten-Johansen J, Yellon DM and Garcia-Dorado D. Ischaemic conditioning and targeting reperfusion injury: a 30 year voyage of discovery. *Basic Res Cardiol.* 2016;111:70.
11. Methner C, Lukowski R, Grube K, Loga F, Smith RA, Murphy MP, Hofmann F and Krieg T. Protection through postconditioning or a mitochondria-targeted S-nitrosothiol is unaffected by cardiomyocyte-selective ablation of protein kinase G. *Basic Res Cardiol.* 2013;108:337.
12. Jin C, Wu J, Watanabe M, Okada T and Iesaki T. Mitochondrial K<sup>+</sup> channels are involved in ischemic postconditioning in rat hearts. *J Physiol Sci.* 2012;62:325-332.
13. Staat P, Rioufol G, Piot C, Cottin Y, Cung TT, L'Huillier I, Aupetit JF, Bonnefoy E, Finet G, Andre-Fouet X and Ovize M. Postconditioning the human heart. *Circulation.* 2005;112:2143-2148.
14. Laskey WK, Yoon S, Calzada N and Ricciardi MJ. Concordant improvements in coronary flow reserve and ST-segment resolution during percutaneous coronary intervention for acute myocardial infarction: a benefit of postconditioning. *Catheter Cardiovasc Interv.* 2008;72:212-220.
15. Xue F, Yang X, Zhang B, Zhao C, Song J, Jiang T and Jiang W. Postconditioning the human heart in percutaneous coronary intervention. *Clin Cardiol.* 2010;33:439-444.

16. Hahn JY, Song YB, Kim EK, Yu CW, Bae JW, Chung WY, Choi SH, Choi JH, Bae JH, An KJ, Park JS, Oh JH, Kim SW, Hwang JY, Ryu JK, Park HS, Lim DS and Gwon HC. Ischemic postconditioning during primary percutaneous coronary intervention: the effects of postconditioning on myocardial reperfusion in patients with ST-segment elevation myocardial infarction (POST) randomized trial. *Circulation*. 2013;128:1889-1896.
17. Sorensson P, Saleh N, Bouvier F, Bohm F, Settergren M, Caidahl K, Tornvall P, Arheden H, Ryden L and Pernow J. Effect of postconditioning on infarct size in patients with ST elevation myocardial infarction. *Heart*. 2010;96:1710-1715.
18. Freixa X, Bellera N, Ortiz-Perez JT, Jimenez M, Pare C, Bosch X, De Caralt TM, Betriu A and Masotti M. Ischaemic postconditioning revisited: lack of effects on infarct size following primary percutaneous coronary intervention. *Eur Heart J*. 2012;33:103-112.
19. Tarantini G, Favaretto E, Marra MP, Frigo AC, Napodano M, Cacciavillani L, Giovagnoni A, Renda P, De Biasio V, Plebani M, Mion M, Zaninotto M, Isabella G, Bilato C and Iliceto S. Postconditioning during coronary angioplasty in acute myocardial infarction: the POST-AMI trial. *Int J Cardiol*. 2012;162:33-38.
20. Hausenloy DJ, Botker HE, Engstrom T, Erlinge D, Heusch G, Ibanez B, Kloner RA, Ovize M, Yellon DM and Garcia-Dorado D. Targeting reperfusion injury in patients with ST-segment elevation myocardial infarction: trials and tribulations. *Eur Heart J*. 2017;38:935-941.
21. Heusch G and Rassaf T. Time to Give Up on Cardioprotection? A Critical Appraisal of Clinical Studies on Ischemic Pre-, Post-, and Remote Conditioning. *Circ Res*. 2016;119:676-695.
22. Methner C, Buonincontri G, Hu CH, Vujic A, Kretschmer A, Sawiak S, Carpenter A, Stasch JP and Krieg T. Riociguat reduces infarct size and post-infarct heart failure in mouse hearts: insights from MRI/PET imaging. *PLoS One*. 2013;8:e83910.
23. Salloum FN, Das A, Samidurai A, Hoke NN, Chau VQ, Ockaili RA, Stasch JP and Kukreja RC. Cinaciguat, a novel activator of soluble guanylate cyclase, protects against ischemia/reperfusion injury: role of hydrogen sulfide. *Am J Physiol Heart Circ Physiol*. 2012;302:H1347-1354.
24. Salloum FN, Takenoshita Y, Ockaili RA, Daoud VP, Chou E, Yoshida K and Kukreja RC. Sildenafil and vardenafil but not nitroglycerin limit myocardial infarction through opening of mitochondrial K(ATP) channels when administered at reperfusion following ischemia in rabbits. *J Mol Cell Cardiol*. 2007;42:453-458.
25. Das A, Salloum FN, Xi L, Rao YJ and Kukreja RC. ERK phosphorylation mediates sildenafil-induced myocardial protection against ischemia-reperfusion injury in mice. *Am J Physiol Heart Circ Physiol*. 2009;296:H1236-1243.
26. Behmenburg F, Dorsch M, Huhn R, Mally D, Heinen A, Hollmann MW and Berger MM. Impact of Mitochondrial Ca<sup>2+</sup>-Sensitive Potassium (mBKCa) Channels in Sildenafil-Induced Cardioprotection in Rats. *PLoS One*. 2015;10:e0144737.
27. Maas O, Donat U, Frenzel M, Rutz T, Kroemer HK, Felix SB and Krieg T. Vardenafil protects isolated rat hearts at reperfusion dependent on GC and PKG. *Br J Pharmacol*. 2008;154:25-31.

28. Salloum FN, Chau VQ, Hoke NN, Abbate A, Varma A, Ockaili RA, Toldo S and Kukreja RC. Phosphodiesterase-5 inhibitor, tadalafil, protects against myocardial ischemia/reperfusion through protein-kinase g-dependent generation of hydrogen sulfide. *Circulation*. 2009;120:S31-36.
29. Costa AD, Garlid KD, West IC, Lincoln TM, Downey JM, Cohen MV and Critz SD. Protein kinase G transmits the cardioprotective signal from cytosol to mitochondria. *Circ Res*. 2005;97:329-336.
30. Costa AD and Garlid KD. Intramitochondrial signaling: interactions among mitoKATP, PKCepsilon, ROS, and MPT. *Am J Physiol Heart Circ Physiol*. 2008;295:H874-882.
31. Costa AD, Pierre SV, Cohen MV, Downey JM and Garlid KD. cGMP signalling in pre- and post-conditioning: the role of mitochondria. *Cardiovasc Res*. 2008;77:344-352.
32. Oldenburg O, Qin Q, Krieg T, Yang XM, Philipp S, Critz SD, Cohen MV and Downey JM. Bradykinin induces mitochondrial ROS generation via NO, cGMP, PKG, and mitoKATP channel opening and leads to cardioprotection. *Am J Physiol Heart Circ Physiol*. 2004;286:H468-476.
33. Singh H, Lu R, Bopassa JC, Meredith AL, Stefani E and Toro L. MitoBK(Ca) is encoded by the *Kcnma1* gene, and a splicing sequence defines its mitochondrial location. *Proc Natl Acad Sci U S A*. 2013;110:10836-10841.
34. Soltysinska E, Bentzen BH, Barthmes M, Hattel H, Thrush AB, Harper ME, Qvortrup K, Larsen FJ, Schiffer TA, Losa-Reyna J, Straubinger J, Kniess A, Thomsen MB, Bruggemann A, Fenske S, Biel M, Ruth P, Wahl-Schott C, Boushel RC, Olesen SP and Lukowski R. KCNMA1 encoded cardiac BK channels afford protection against ischemia-reperfusion injury. *PLoS One*. 2014;9:e103402.
35. Kang SH, Park WS, Kim N, Youm JB, Warda M, Ko JH, Ko EA and Han J. Mitochondrial Ca<sup>2+</sup>-activated K<sup>+</sup> channels more efficiently reduce mitochondrial Ca<sup>2+</sup> overload in rat ventricular myocytes. *Am J Physiol Heart Circ Physiol*. 2007;293:H307-313.
36. Sato T, Saito T, Saegusa N and Nakaya H. Mitochondrial Ca<sup>2+</sup>-activated K<sup>+</sup> channels in cardiac myocytes: a mechanism of the cardioprotective effect and modulation by protein kinase A. *Circulation*. 2005;111:198-203.
37. Chouchani ET, Pell VR, James AM, Work LM, Saeb-Parsy K, Frezza C, Krieg T and Murphy MP. A Unifying Mechanism for Mitochondrial Superoxide Production during Ischemia-Reperfusion Injury. *Cell Metab*. 2016;23:254-263.
38. Bentzen BH, Osadchii O, Jespersen T, Hansen RS, Olesen SP and Grunnet M. Activation of big conductance Ca(2+)-activated K (+) channels (BK) protects the heart against ischemia-reperfusion injury. *Pflugers Arch*. 2009;457:979-988.
39. Wang X, Yin C, Xi L and Kukreja RC. Opening of Ca<sup>2+</sup>-activated K<sup>+</sup> channels triggers early and delayed preconditioning against I/R injury independent of NOS in mice. *Am J Physiol Heart Circ Physiol*. 2004;287:H2070-2077.

40. Wojtovich AP, Sherman TA, Nadtochiy SM, Urciuoli WR, Brookes PS and Nehrke K. SLO-2 is cytoprotective and contributes to mitochondrial potassium transport. *PLoS One*. 2011;6:e28287.
41. Zhou XB, Wulfsen I, Utku E, Sausbier U, Sausbier M, Wieland T, Ruth P and Korth M. Dual role of protein kinase C on BK channel regulation. *Proc Natl Acad Sci U S A*. 2010;107:8005-8010.
42. Swayze RD and Braun AP. A catalytically inactive mutant of type I cGMP-dependent protein kinase prevents enhancement of large conductance, calcium-sensitive K<sup>+</sup> channels by sodium nitroprusside and cGMP. *J Biol Chem*. 2001;276:19729-19737.
43. Kyle BD, Hurst S, Swayze RD, Sheng J and Braun AP. Specific phosphorylation sites underlie the stimulation of a large conductance, Ca<sup>2+</sup>-activated K<sup>(+)</sup> channel by cGMP-dependent protein kinase. *FASEB J*. 2013;27:2027-2038.
44. Sausbier M, Hu H, Arntz C, Feil S, Kamm S, Adelsberger H, Sausbier U, Sailer CA, Feil R, Hofmann F, Korth M, Shipston MJ, Knaus HG, Wolfer DP, Pedroarena CM, Storm JF and Ruth P. Cerebellar ataxia and Purkinje cell dysfunction caused by Ca<sup>2+</sup>-activated K<sup>+</sup> channel deficiency. *Proc Natl Acad Sci U S A*. 2004;101:9474-9478.
45. Agah R, Frenkel PA, French BA, Michael LH, Overbeek PA and Schneider MD. Gene recombination in postmitotic cells. Targeted expression of Cre recombinase provokes cardiac-restricted, site-specific rearrangement in adult ventricular muscle in vivo. *J Clin Invest*. 1997;100:169-179.
46. Sprossmann F, Pankert P, Sausbier U, Wirth A, Zhou XB, Madlung J, Zhao H, Bucurenciu I, Jakob A, Lamkemeyer T, Neuhuber W, Offermanns S, Shipston MJ, Korth M, Nordheim A, Ruth P and Sausbier M. Inducible knockout mutagenesis reveals compensatory mechanisms elicited by constitutive BK channel deficiency in overactive murine bladder. *FEBS J*. 2009;276:1680-1697.
47. Illison J, Tian L, McClafferty H, Werno M, Chamberlain LH, Leiss V, Sassmann A, Offermanns S, Ruth P, Shipston MJ and Lukowski R. Obesogenic and Diabetogenic Effects of High-Calorie Nutrition Require Adipocyte BK Channels. *Diabetes*. 2016;65:3621-3635.
48. Lu R, Lukowski R, Sausbier M, Zhang DD, Sisignano M, Schuh CD, Kuner R, Ruth P, Geisslinger G and Schmidtke A. BKCa channels expressed in sensory neurons modulate inflammatory pain in mice. *Pain*. 2014;155:556-565.
49. Wirth A, Benyo Z, Lukasova M, Leutgeb B, Wettschureck N, Gorbey S, Orsy P, Horvath B, Maser-Gluth C, Greiner E, Lemmer B, Schutz G, Gutkind JS and Offermanns S. G12-G13-LARG-mediated signaling in vascular smooth muscle is required for salt-induced hypertension. *Nat Med*. 2008;14:64-68.
50. Muzumdar MD, Tasic B, Miyamichi K, Li L and Luo L. A global double-fluorescent Cre reporter mouse. *Genesis*. 2007;45:593-605.
51. Cocheme HM, Quin C, McQuaker SJ, Cabreiro F, Logan A, Prime TA, Abakumova I, Patel JV, Fearnley IM, James AM, Porteous CM, Smith RA, Saeed S, Carre JE, Singer M, Gems D, Hartley RC, Partridge L and Murphy MP. Measurement of H<sub>2</sub>O<sub>2</sub> within living *Drosophila*

- during aging using a ratiometric mass spectrometry probe targeted to the mitochondrial matrix. *Cell Metab.* 2011;13:340-350.
52. Fliss H and Gattinger D. Apoptosis in ischemic and reperfused rat myocardium. *Circ Res.* 1996;79:949-956.
53. Hausenloy DJ, Tsang A and Yellon DM. The reperfusion injury salvage kinase pathway: a common target for both ischemic preconditioning and postconditioning. *Trends Cardiovasc Med.* 2005;15:69-75.
54. Nagata T, Yasukawa H, Kyogoku S, Oba T, Takahashi J, Nohara S, Minami T, Mawatari K, Sugi Y, Shimozono K, Pradervand S, Hoshijima M, Aoki H, Fukumoto Y and Imaizumi T. Cardiac-Specific SOCS3 Deletion Prevents In Vivo Myocardial Ischemia Reperfusion Injury through Sustained Activation of Cardioprotective Signaling Molecules. *PLoS One.* 2015;10:e0127942.
55. Clark AG, Hall SK and Shipston MJ. ATP inhibition of a mouse brain large-conductance K<sup>+</sup> (mslo) channel variant by a mechanism independent of protein phosphorylation. *J Physiol.* 1999;516 ( Pt 1):45-53.
56. Mizuguchi Y, Oishi Y, Miyoshi H, Iuchi A, Nagase N and Oki T. The functional role of longitudinal, circumferential, and radial myocardial deformation for regulating the early impairment of left ventricular contraction and relaxation in patients with cardiovascular risk factors: a study with two-dimensional strain imaging. *J Am Soc Echocardiogr.* 2008;21:1138-1144.
57. Bauer M, Cheng S, Jain M, Ngoy S, Theodoropoulos C, Trujillo A, Lin FC and Liao R. Echocardiographic speckle-tracking based strain imaging for rapid cardiovascular phenotyping in mice. *Circ Res.* 2011;108:908-916.
58. Ferdinandy P, Schulz R and Baxter GF. Interaction of cardiovascular risk factors with myocardial ischemia/reperfusion injury, preconditioning, and postconditioning. *Pharmacol Rev.* 2007;59:418-458.
59. Wojtovich AP, Nadtochiy SM, Urciuoli WR, Smith CO, Grunnet M, Nehrke K and Brookes PS. A non-cardiomyocyte autonomous mechanism of cardioprotection involving the SLO1 BK channel. *PeerJ.* 2013;1:e48.
60. Suleiman MS, Halestrap AP and Griffiths EJ. Mitochondria: a target for myocardial protection. *Pharmacol Ther.* 2001;89:29-46.
61. Pell VR, Chouchani ET, Murphy MP, Brookes PS and Krieg T. Moving Forwards by Blocking Back-Flow: The Yin and Yang of MI Therapy. *Circ Res.* 2016;118:898-906.
62. Pain T, Yang XM, Critz SD, Yue Y, Nakano A, Liu GS, Heusch G, Cohen MV and Downey JM. Opening of mitochondrial K(ATP) channels triggers the preconditioned state by generating free radicals. *Circ Res.* 2000;87:460-466.
63. Miro-Casas E, Ruiz-Meana M, Agullo E, Stahlhofen S, Rodriguez-Sinovas A, Cabestrero A, Jorge I, Torre I, Vazquez J, Boengler K, Schulz R, Heusch G and Garcia-Dorado D. Connexin43 in cardiomyocyte mitochondria contributes to mitochondrial potassium uptake. *Cardiovasc Res.* 2009;83:747-756.



64. Boengler K, Ungefug E, Heusch G, Leybaert L and Schulz R. Connexin 43 impacts on mitochondrial potassium uptake. *Front Pharmacol*. 2013;4:73.
65. Heinzl FR, Luo Y, Li X, Boengler K, Buechert A, Garcia-Dorado D, Di Lisa F, Schulz R and Heusch G. Impairment of diazoxide-induced formation of reactive oxygen species and loss of cardioprotection in connexin 43 deficient mice. *Circ Res*. 2005;97:583-586.
66. Stowe DF, Aldakkak M, Camara AK, Riess ML, Heinen A, Varadarajan SG and Jiang MT. Cardiac mitochondrial preconditioning by Big Ca<sup>2+</sup>-sensitive K<sup>+</sup> channel opening requires superoxide radical generation. *Am J Physiol Heart Circ Physiol*. 2006;290:H434-440.
67. Aon MA, Cortassa S, Wei AC, Grunnet M and O'Rourke B. Energetic performance is improved by specific activation of K<sup>+</sup> fluxes through K(Ca) channels in heart mitochondria. *Biochim Biophys Acta*. 2010;1797:71-80.
68. Hausenloy DJ and Yellon DM. Reperfusion injury salvage kinase signalling: taking a RISK for cardioprotection. *Heart Fail Rev*. 2007;12:217-234.
69. Skyschally A, Gent S, Amanakis G, Schulte C, Kleinbongard P and Heusch G. Across-Species Transfer of Protection by Remote Ischemic Preconditioning With Species-Specific Myocardial Signal Transduction by Reperfusion Injury Salvage Kinase and Survival Activating Factor Enhancement Pathways. *Circ Res*. 2015;117:279-288.
70. Skyschally A, van Caster P, Boengler K, Gres P, Musiolik J, Schilawa D, Schulz R and Heusch G. Ischemic postconditioning in pigs: no causal role for RISK activation. *Circ Res*. 2009;104:15-18.
71. Miura T and Tanno M. The mPTP and its regulatory proteins: final common targets of signalling pathways for protection against necrosis. *Cardiovasc Res*. 2012;94:181-189.
72. Liu Y, Sato T, O'Rourke B and Marban E. Mitochondrial ATP-dependent potassium channels: novel effectors of cardioprotection? *Circulation*. 1998;97:2463-2469.
73. Wang X, Fisher PW, Xi L and Kukreja RC. Essential role of mitochondrial Ca<sup>2+</sup>-activated and ATP-sensitive K<sup>+</sup> channels in sildenafil-induced late cardioprotection. *J Mol Cell Cardiol*. 2008;44:105-113.
74. Lukowski R, Krieg T, Rybalkin SD, Beavo J and Hofmann F. Turning on cGMP-dependent pathways to treat cardiac dysfunctions: boom, bust, and beyond. *Trends Pharmacol Sci*. 2014;35:404-413.
75. Tirziu D, Giordano FJ and Simons M. Cell communications in the heart. *Circulation*. 2010;122:928-937.
76. Korkmaz-Icoz S, Radovits T and Szabo G. Targeting phosphodiesterase 5 as a therapeutic option against myocardial ischaemia/reperfusion injury and for treating heart failure. *Br J Pharmacol*. 2017. doi: 10.1111/bph.13749
77. Sausbier M, Arntz C, Bucurenciu I, Zhao H, Zhou XB, Sausbier U, Feil S, Kamm S, Essin K, Sailer CA, Abdullah U, Krippeit-Drews P, Feil R, Hofmann F, Knaus HG, Kenyon C, Shipston MJ, Storm JF, Neuhuber W, Korth M, Schubert R, Gollasch M and Ruth P. Elevated blood pressure linked to primary hyperaldosteronism and impaired vasodilation in BK channel-deficient mice. *Circulation*. 2005;112:60-68.

## Figure Legends

### Figure 1. Hearts globally lacking BK are more vulnerable to ischemia and reperfusion injury and are not protected by ischemic postconditioning maneuvers

(A) Risk zones (shown as percentage of the respective total heart areas) did not differ between global BK-KO (BK<sup>-/-</sup>) and BK-WT (BK<sup>+/+</sup>) mice subjected to different experimental setups *i.e.* after 30 min ischemia followed by 120 min reperfusion (I/R), sham-operation without ligation of the coronary artery (I/R *sham*) or a postconditioning (*iPost*) protocol consisting of six consecutive cycles of reperfusion and re-occlusion directly after the ischemic period (I/R + *iPost*) (Suppl. Fig. 1, ①-③). (B) Infarct size is expressed as percentage of the risk zone and was significantly increased in BK<sup>-/-</sup> (n=11) in comparison to litter-matched BK<sup>+/+</sup> (n=8) mice after I/R (left). As expected, *sham*-surgery did not cause myocardial infarction in both genotypes (middle, n=6 per genotype). A significant reduction in infarct size was observed in BK<sup>+/+</sup> hearts (n=8) subjected to *iPost*, whereas BK<sup>-/-</sup> hearts (n=9) did not respond to this cardioprotective maneuver (right). Representative Evan's Blue and TTC double-stained heart slices of the two genotypes subjected to different I/R setups are shown in the lower panel (blue: unaffected heart muscle; red plus white: risk zone; white: infarcted tissue; note: some slices showed a central white spot reflecting the ventricular lumen). (C) Serum levels of cardiac Troponin I (cTnI) determined at the end of reperfusion correlate well with the infarct sizes (n=8 for BK<sup>+/+</sup> (I/R); n=11 for BK<sup>-/-</sup> (I/R) and n=6 for both genotypes (I/R *sham*)). (D) Cell rounding and blebbing as common characteristics of hypercontracted CM undergoing cell death *in vitro* (black arrowhead) were more often observed in BK<sup>-/-</sup> CMs after 90 min of hypoxia. (E) Under hypoxic conditions lactate dehydrogenase (LDH) release rates showed a clear tendency towards higher values in BK<sup>-/-</sup>

compared to BK<sup>+/+</sup> CM cultures (*normoxia*: n=19 for BK<sup>+/+</sup> and n=17 for BK<sup>-/-</sup>; *hypoxia*: n=17 for BK<sup>+/+</sup> and n=18 for BK<sup>-/-</sup>).

All data were assessed using two-way ANOVA followed by Bonferroni-corrected Student's t-tests, except for (B+C) groups were compared by Welch's t-test due to unequal variance and for (E) the Kruskal-Wallis test followed by Dunn's test for multiple pairwise comparisons was performed with \*p<0.05, \*\*\*p<0.001 for the comparison between BK<sup>-/-</sup> and BK<sup>+/+</sup> groups; §: p<0.01, #: p<0.001 for the comparison to the respective I/R group.

**Figure 2. Cardiomyocyte-specific ablation of the BK channel using the  $\alpha$ MHC-Cre<sup>Tg/+</sup> recombination system**



(A) Crossbreeding of mice carrying the  $\alpha$ MHC-Cre recombinase ( $\alpha$ MHC-Cre<sup>Tg/+</sup>) with global double-fluorescent Cre reporter mice (ROSA<sup>mTG/+</sup>) established a high efficacy of target DNA recombination as indicated by the switch from cell membrane-localized red fluorescence (mT) to membrane-localized green fluorescence (mG) protein. In Cre-negative ( $\alpha$ MHC-Cre<sup>+/+</sup>) ROSA<sup>mTG/+</sup> mice all cardiac cells continued to express mT. DAPI was used as a nuclear counterstain. (B) CMs were evaluated for the expression of mT (red) or mG (green) in  $\alpha$ MHC-Cre<sup>Tg/+</sup>; ROSA<sup>mTG/+</sup> double-transgenic heart sections (n=1652 counted cells in total derived from n=4 mice) in order to quantify the recombination efficiency. (C) Genomic PCR analysis of the  $\alpha$ MHC-Cre<sup>Tg/+</sup>-mediated recombination of the floxed BK gene locus in different tissues obtained from  $\alpha$ MHC-Cre<sup>Tg/+</sup>; CMBK<sup>+/fl</sup> mice. The PCR products were amplified by BK-specific primers derived from the floxed (*fl*), wild type (+), or knock-out (-) allele. A somatic conversion of the floxed allele to the (-) allele was only observed in cardiac tissue. The size of the PCR amplicons were 577 bp, 466 bp and 132 bp for the (*fl*), (+) and (-) allele. The pore-

forming  $\alpha$ -subunit of the BK channel was identified in mitochondrial protein fractions obtained from CMBK-CTR (CMBK<sup>+fl</sup>) CMs using either (D) custom-made or (E) commercial antibodies for the BK  $\alpha$ -subunit.

**Figure 3. CMBK mutant mice present with an impaired heart function and a decreased blood pressure**

(A) Fractional shortening (FS, %), (B) ejection fraction (EF, %) and (C) heart rate were slightly but significantly reduced in cardiomyocyte-specific BK knockout (CMBK<sup>-fl</sup>, n=9) as compared to litter-matched control mice (CMBK<sup>+fl</sup>, n=8). (D) Mean arterial blood pressure (MAP) measured for 48 hours was decreased in CMBK<sup>-fl</sup> (n=10) versus CMBK<sup>+fl</sup> mice (n=7). (E) No difference was seen in pulse pressure between genotypes.

Data of (A) - (C) and (E) were analyzed using the Student's t-test and significance levels in (D) were tested using repeated measures ANOVA followed by Bonferroni post-hoc test, all with \*p<0.05, \*\*p<0.01 for CMBK<sup>-fl</sup> vs. CMBK<sup>+fl</sup>.

**Figure 4. Cardiac damage due to apoptotic cell death and lower p-ERK/p-AKT levels may be responsible for larger infarct sizes of mice with a CM-specific deletion of the BK channel**

(A) Risk zones were not different between CMBK-CTR (CMBK<sup>+fl</sup>) and CMBK-KO (CMBK<sup>-fl</sup>) mice. (B) Infarct sizes after I/R, expressed as percentage of the risk zone, were significantly increased in the absence of CMBK channels, whereas *sham*-surgery did not result in myocardial damage. Representative heart slices are shown below their respective genotype and treatment group. (C) Serum levels of cardiac Troponin I (cTnI) collected from CMBK-CTR (CMBK<sup>+fl</sup>)

and CMBK-KO (CMBK<sup>-fl</sup>) mice directly after the I/R (n=8 for I/R and n=4 for I/R *sham* per genotype). **(D)** Baseline normalized ratio of MitoP/MitoB as a marker for ROS abundance after I/R in CMBK<sup>+fl</sup> and CMBK<sup>-fl</sup> (n=8 per genotype). **(E)** Overview of the 8 equidistant cardiac regions which were analyzed in-depth after ligation (black arrow). **(F)** Representative TUNEL images from region 3 of CMBK<sup>+fl</sup> and CMBK<sup>-fl</sup> hearts. **(G)** TUNEL quantification of the 8 equidistant cardiac regions from CMBK<sup>+fl</sup> and CMBK<sup>-fl</sup> hearts after I/R (n=3 per genotype). Phosphorylation of the pro-survival kinases **(H)** ERK and **(I)** Akt was elevated in CMBK<sup>+fl</sup> mice after 30 min ischemia followed by 10 min of reperfusion compared to CMBK<sup>-fl</sup> mice (n=4 per genotype). Representative immunoblots for p-ERK/ERK and p-Akt/Akt are shown below the respective panels.



Data presented in (A), (B), (H) and (I) were analyzed using two-way ANOVA followed by Bonferroni-corrected Student's t-tests. Data in (C) were compared by Welch's t-test for unequal variances and levels of significance in (D) were tested with the Mann-Whitney-U-test. In (G) a pairwise comparison was performed for each heart region using the Student's t-test. Significance levels are indicated with \*p<0.05, \*\*p<0.01, \*\*\*p<0.001 CMBK<sup>-fl</sup> vs. CMBK<sup>+fl</sup> and §: p<0.01 #: p<0.001 to respective I/R group.

### **Figure 5. Mechanical interventions and cardioprotective effects of pharmacological BK modulators during I/R require BK in CM**

**(A)** Postconditioning (*iPost*) as well as preconditioning (*iPre*; Suppl. Fig. 1, **3** + **4**) significantly reduced infarct size (shown as percentage of the risk zone) by I/R in CMBK-CTR (CMBK<sup>+fl</sup>) mice. The protective effect of both interventions was largely attenuated in CMBK-KO mice (CMBK<sup>-fl</sup>). **(B)** Comparison of the percentage reduction in infarct size after *iPost*

between global and CM-specific BK knockout mutants and their corresponding litter-matched controls *i.e.* WT and CMBK<sup>+fl</sup> mice. Values were calculated from the baseline I/R injury of the respective groups (see Fig. 1B+4B). (C) The BK channel blocker paxilline (*PAX*; Suppl. Fig. 1, 5) increased the I/R injury in CMBK<sup>+fl</sup> mice to CMBK<sup>-fl</sup> levels, whereas the BK channel opener NS11021 (Suppl. Fig. 1, 6) opposed the cardiac damage by a CM-specific BK channel pathway. (D) Changes in infarct size displayed in percent of the I/R injury (see Fig. 4B) after administration of paxilline or NS11021. Representative heart slices of the respective genotype and setup are shown in the lower part of panel (A) and (C) with n=8 mice used per genotype and setup.

All data were examined using two-way ANOVA followed by Bonferroni-corrected Student's *t*-tests with \*\*\**p*<0.001 CMBK<sup>-fl</sup> vs. CMBK<sup>+fl</sup>; †: *p*<0.05, #: *p*<0.001 to respective I/R group and †<sub>2</sub>: *p*<0.05, §<sub>1/2</sub>: *p*<0.01 to respective control treatment group (Suppl. Fig. 3D).

### Figure 6. Cardioprotective effects of NO-GC activators/stimulators and PDE5 inhibitors depend on CM-specific BKs

(A) Infarction is expressed as percentage of the risk zone and was significantly reduced after injection of the NO-GC stimulator riociguat (*RIO*) or the NO-GC activator cinaciguat (*CIN*) in CMBK-CTR mice (CMBK<sup>+fl</sup>, n=8 each). Cardioprotection afforded with riociguat was attenuated and abolished for cinaciguat in CMBK-KO mice (CMBK<sup>-fl</sup>, *RIO*: n=10, *CIN*: n=8). (B) Reduction (%) in infarct size after administration of riociguat and cinaciguat compared to baseline I/R injury (see Fig. 4B). (C) Injection of the PDE5 blockers sildenafil (*SIL*, n=8 per genotype) and tadalafil (*TAD*, n=9 per genotype) resulted in a significant reduction in infarct size in CMBK<sup>+fl</sup> but not in CMBK<sup>-fl</sup> mice. (D) Reduction (%) in infarct size after treatment with

sildenafil and tadalafil compared to baseline I/R injury (Fig. 4B). (E) CMBK<sup>+fl</sup> did not respond to the cardioprotective stimulus elicited by iPost or SIL after pretreatment with the NO synthase blocker N<sub>ω</sub>-nitro-L-arginine methyl ester (L-NAME) (n=8 per genotype and setup). (F) Alterations in infarct size (in % of I/R (see Fig. 4B)) after L-NAME co-treatment in comparison to I/R + iPost (or SIL) without L-NAME administration (Fig. 5B+6D). Representative heart slices of the respective genotype and setup are shown in the lower panel of (A), (C) and (E). Pharmacological pre- and post-conditioning protocols (A-F) are summarized in Suppl. Fig. 1, 7 + 11). All data were analyzed using two-way ANOVA followed by Bonferroni-corrected Student's t-tests with \*\*\*p<0.001 CMBK<sup>-fl</sup> vs. CMBK<sup>+fl</sup>; †: p<0.05, #: p<0.001 to respective I/R group and §<sub>4</sub>: p<0.01, #<sub>3</sub>: p<0.001 to respective control treatment group (Suppl. Fig. 3E).

### Figure 7. cGMP/cGKI directly modulate mitochondrial BK channels in isolated membrane patches

(A) The cGKI protein was detectable in purified cardiomyocyte mitochondria (CMM) protein extracts, whereas  $\alpha$ -tubulin used as control protein for the co-purified cytoplasmic supernatant was not detectable in the mitochondrial fraction. As compared to total heart lysates (HL) from BK-WT (BK<sup>+/+</sup>) and BK-KO (BK<sup>-/-</sup>) mice, heat shock protein 60 (hsp60) a chaperone specific to the mitochondria was significantly enriched in the protein lysates generated from CMM. Data are representative of three independent experiments. For further information consult Suppl. Fig. 14

(B) Current-voltage (I-V) plot of the single channel activity shown in (C). The single channel conductance calculated from the slope equates 145 pS. (C) A typical BK channel activity in inside-out patches purified from BK-WT CMs. Recordings were performed in 20 mV steps from -60 to +60 mV of the inner mitochondrial membrane potential. (D) Electro-pharmacological

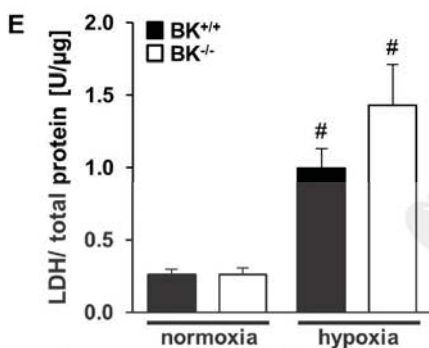
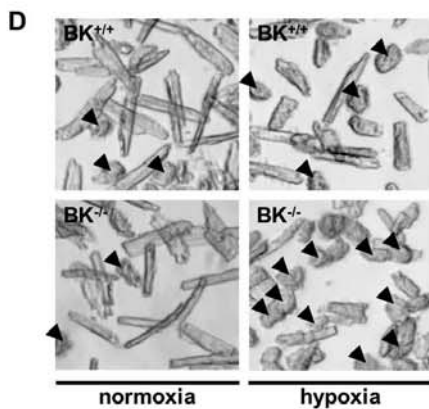
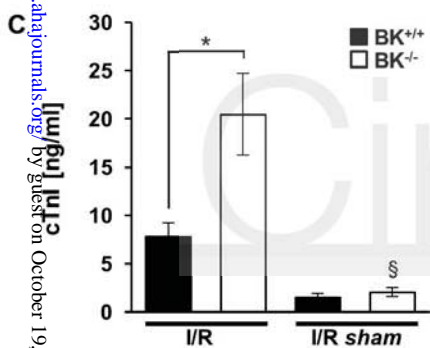
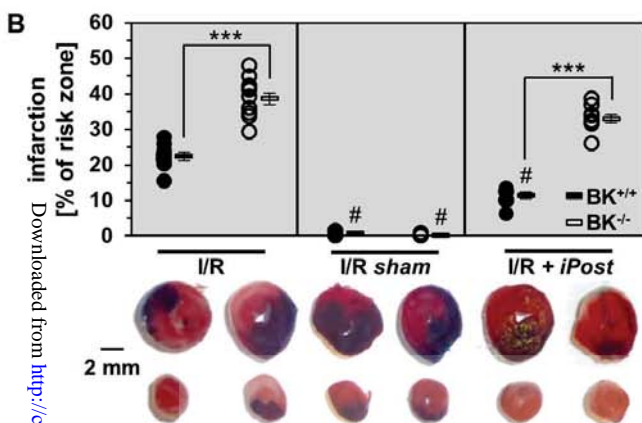
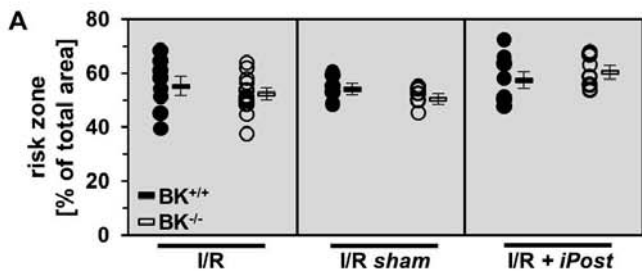
profile of the mitochondrial BK at +60 mV displayed a moderate sensitivity to  $\text{Ca}^{2+}$ . The average probability of opening ( $P_o$ ) declined from 0.54 to 0.28 in the presence of 100  $\mu\text{M}$   $\text{Ca}^{2+}$  (control) or 1  $\mu\text{M}$   $\text{Ca}^{2+}$  (low  $\text{Ca}^{2+}$ ), respectively (left panel). Addition of NS11201 (10  $\mu\text{M}$ ) resulted in an increase in BK channel  $P_o$  from 0.54 (control) to 0.92, whereas the subsequent addition of paxilline (10  $\mu\text{M}$ ) reduced the  $P_o$  to 0.04 (right panel). Open probabilities were calculated from the channel activity observed in 3 or more independent patches. **(E)** A representative trace of BK activity in an IMM patch. After recording a channel activity under control conditions patches were perfused with a solution containing 0.4 mM  $\text{Mg}^{2+}/\text{ATP}$ , which resulted in a small but significant reduction of the channel activity. Subsequent perfusion with the same solution containing 8-Br-cGMP (10  $\mu\text{M}$ ) and cGKI (50 nM) substantially increased  $P_o$ . Paxilline (PAX) almost completely blocked the respective BK channel activity. **(F)** Summary of experiments carried out according to the scheme shown in (E). 8-Br-cGMP/cGKI activated a channel of 145 pS conductance ascribed to the mitochondrial BK in BK-WT ( $\text{BK}^{+/+}$ ; left panel) mitoplasts. Importantly, a rather frequently observed conductance of 95 pS in the BK-KO ( $\text{BK}^{-/-}$ ; right panel) mitoplast patches did not respond to any of the shown treatments. The mean  $\pm$ SEM from 5 or 3 independent recordings in symmetrical 150mM KCl, 0.1 mM  $\text{CaCl}_2$ , 10 mM HEPES, pH=7.2 is shown (unless indicated otherwise) for the 145 pS channel and the 95 pS channel activities, respectively. Data in (D) and (F) were examined using one-way ANOVA with  $*p<0.05$  and  $***p<0.001$ . In the interest of clarity, statistical significances between the paxilline groups in (D, right) and (F, left) and the other recording conditions were not indicated in the respective panels ( $***p<0.001$  for PAX compared to control, NS11201,  $\text{Mg}^{2+}/\text{ATP}$ , and  $\text{Mg}^{2+}/\text{ATP}/8\text{-Br-cGMP}/\text{cGKI}$ ).



**Figure 8. Compromised heart function 4 weeks after myocardial infarction in CMBK-KO mice**

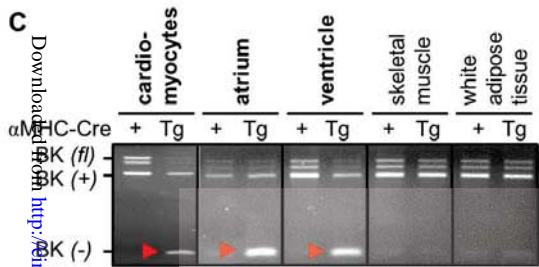
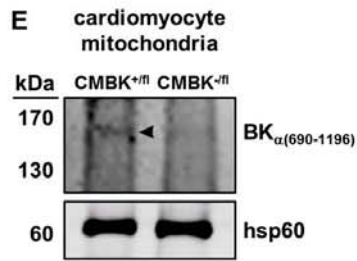
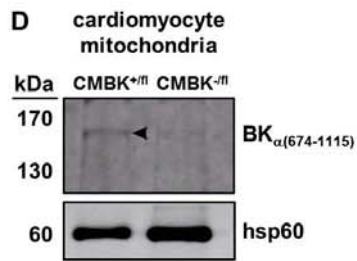
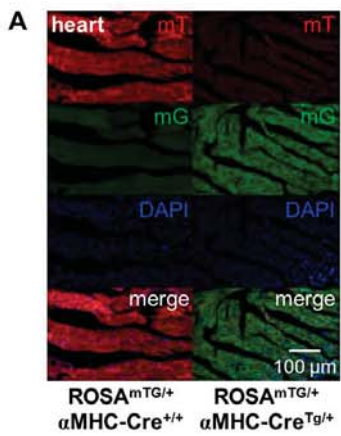
(A) Alterations in the longitudinal strain (%) represent an early marker for cardiac dysfunction after myocardial infarction;<sup>56, 57</sup> abbreviations used: *syst*: systole, *diast*: diastole. (B) Average longitudinal strain was significantly impaired after 30 min ischemia followed by 4 weeks reperfusion (I/R<sub>4wk</sub>) in CMBK-KO (CMBK<sup>-fl</sup>) compared to their litter-matched controls (CMBK<sup>+fl</sup>) (n=13 per genotype). Compared to basal levels both genotypes showed a decreased deformation capacity (#: p<0.001, Suppl. Fig. 16E). Because the end diastolic value was set to zero, negative values of the longitudinal strain indicated a superior systolic contraction of the heart muscle. Typical echocardiographic recordings for the longitudinal strain are shown in Suppl. Fig. 16A-D. (C) Ejection fraction (EF, %) was reduced 4 weeks post-MI compared to basal heart function (#:p<0.001, Suppl. Fig. 16F) without apparent differences between CMBK<sup>-fl</sup> (n=12) and CMBK<sup>+fl</sup> (n=11). (D) Fibrosis (%) was significantly elevated in CMBK<sup>-fl</sup> (n=13) compared to control mice (n=12). Representative micrographs of Sirius red stained heart slices (right) after I/R<sub>4wks</sub> showing the amount of scar formation in both genotypes.

Bars show means ± SEM; data in (B) and (C) were assessed using Student's t-test and (D) was analyzed using the Mann-Whitney-U-test, all with \*p<0.05, \*\*p<0.01 CMBK<sup>-fl</sup> vs. CMBK<sup>+fl</sup>.

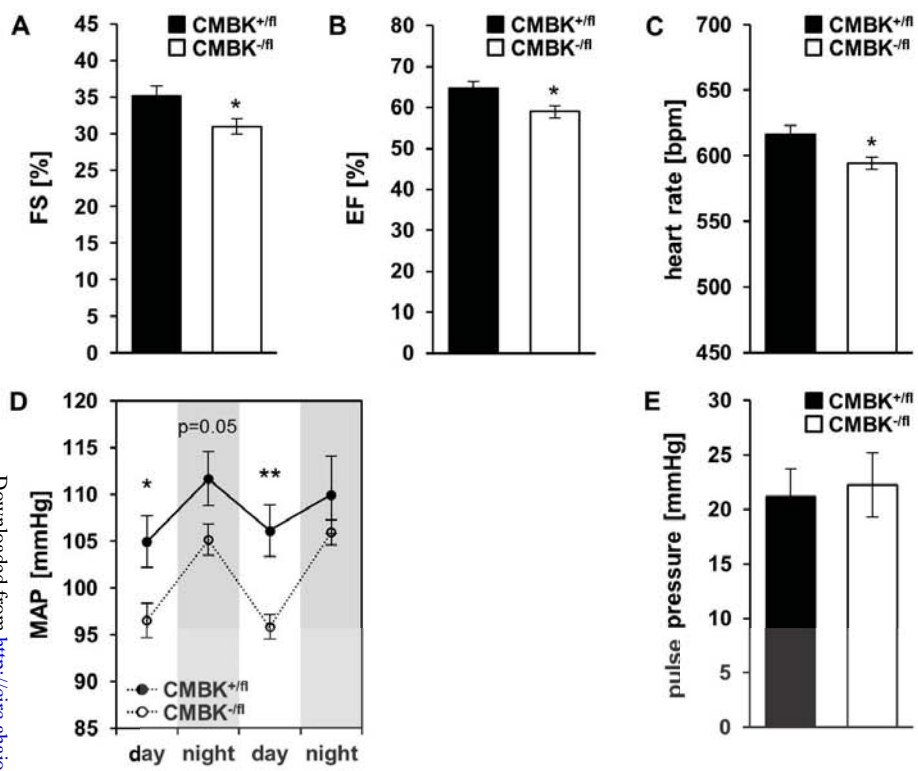


American Heart Association

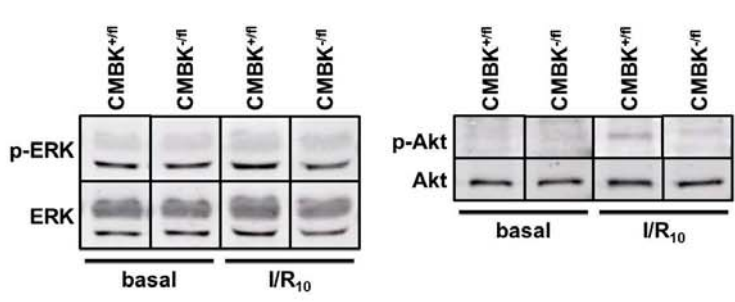
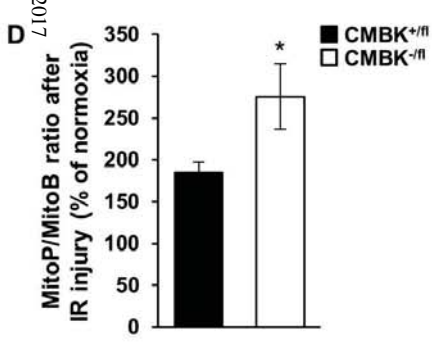
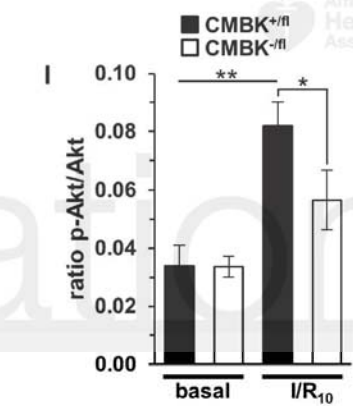
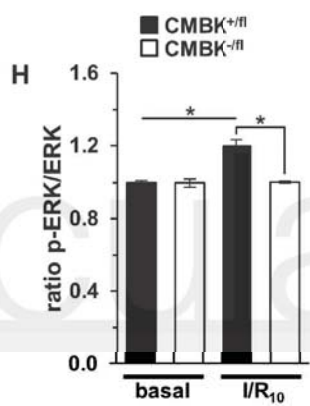
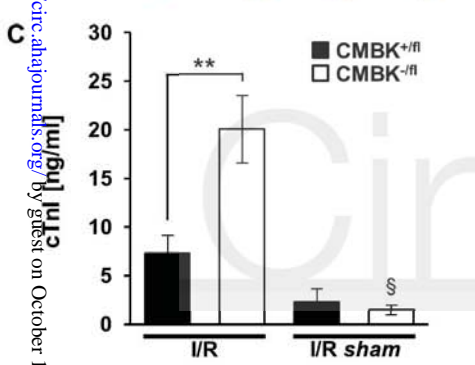
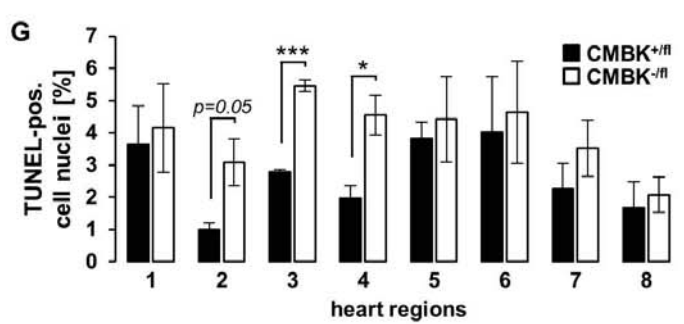
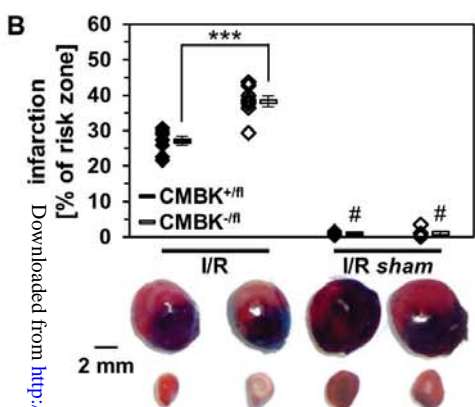
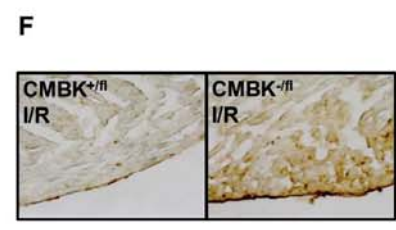
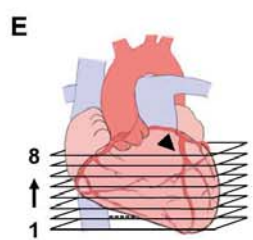
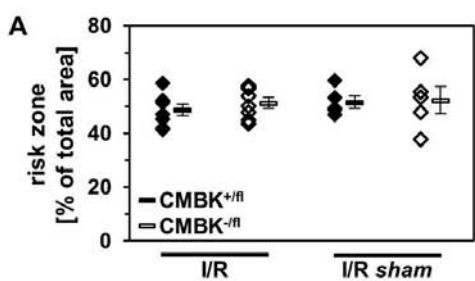
Circulation



Circulation

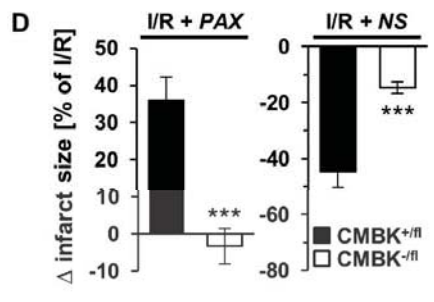
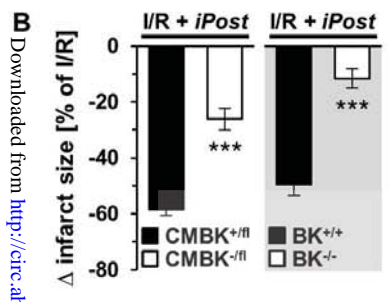
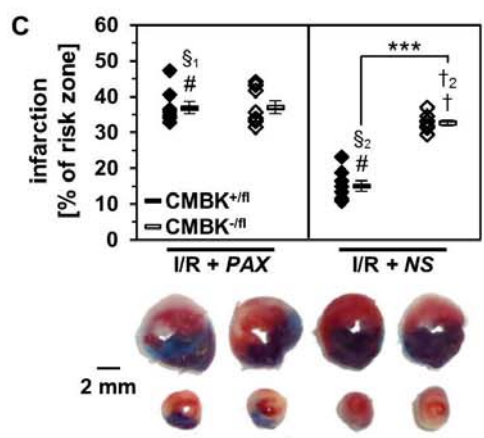
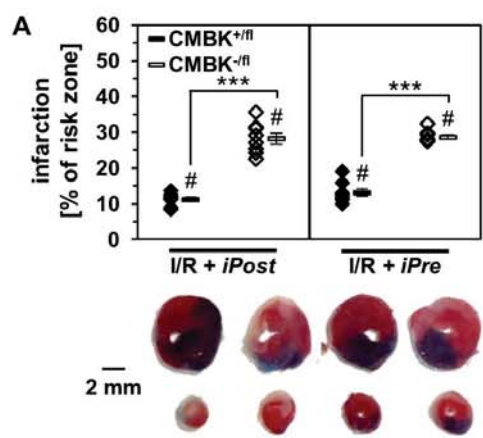


# Circulation

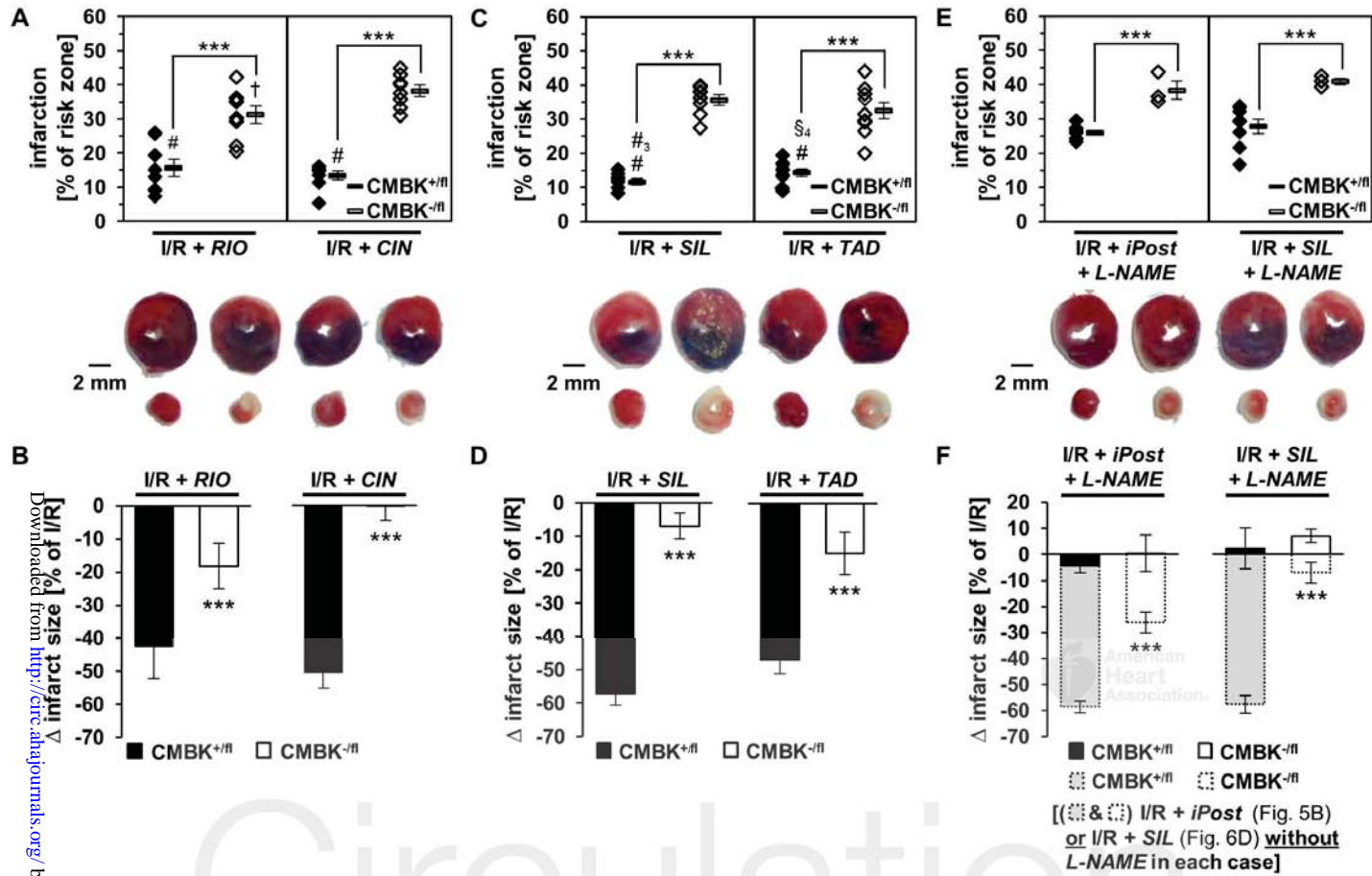


Downloaded from <http://circ.ahajournals.org/> by guest on October 19, 2017

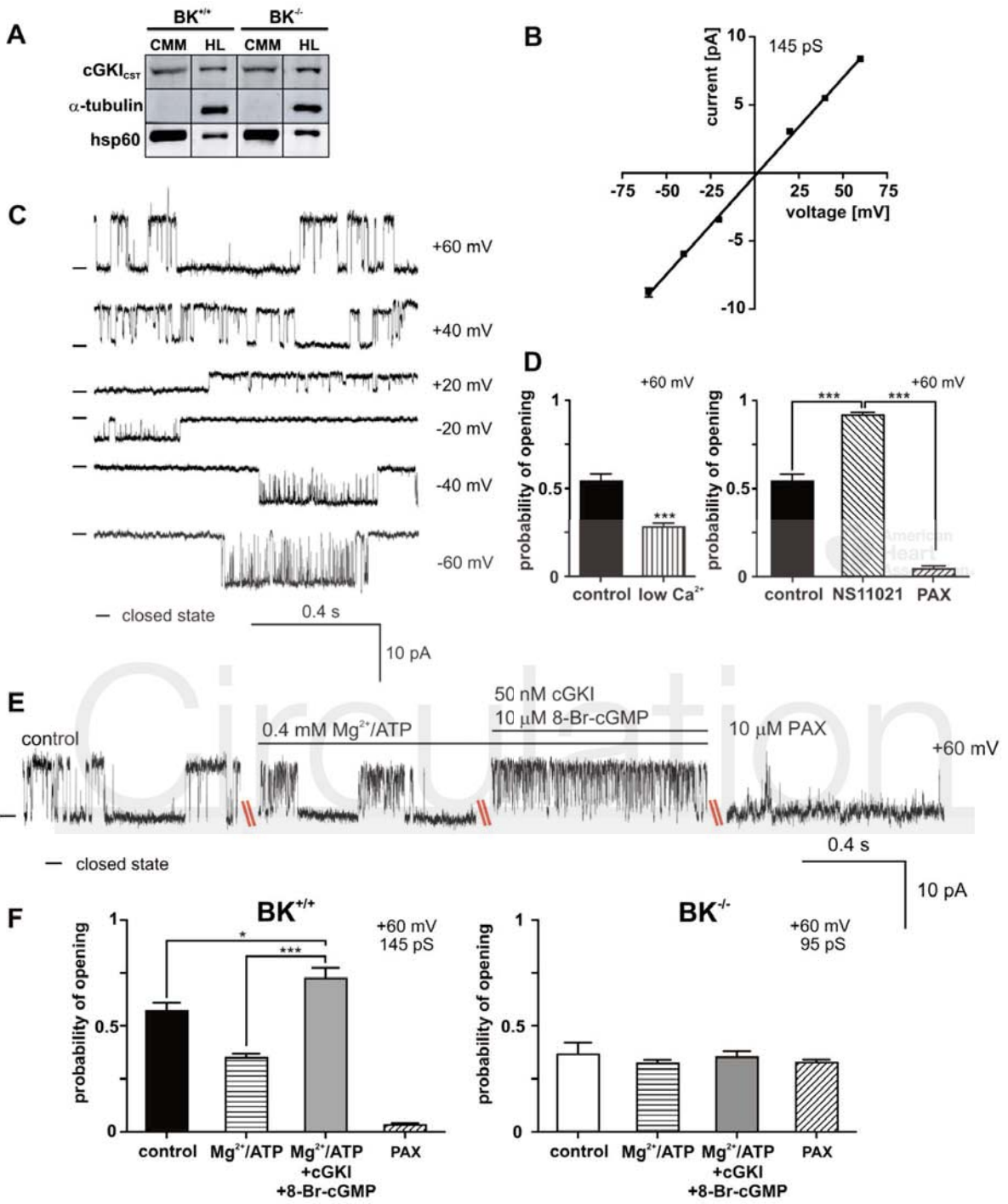




# Circulation

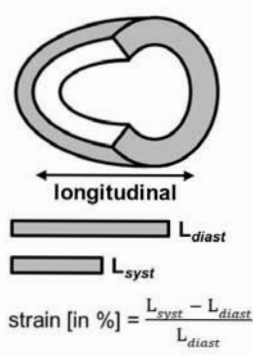


Circulation

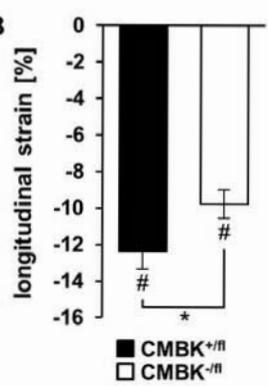




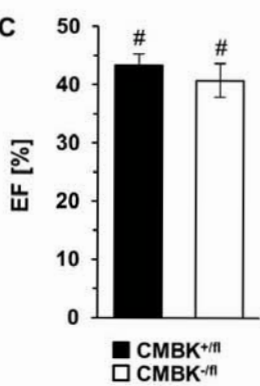
A



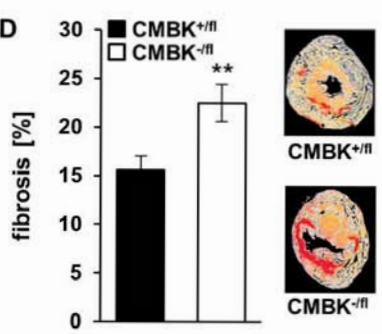
B



C



D



## cGMP-Elevating Compounds and Ischemic Conditioning Provide Cardioprotection Against Ischemia and Reperfusion Injury via Cardiomyocyte-Specific BK Channels

Sandra Frankenreiter, Piotr Bednarczyk, Angelina Kniess, Nadja Bork, Julia Straubinger, Piotr Koprowski, Antoni Wrzosek, Eva Mohr, Angela Logan, Michael P. Murphy, Meinrad Gawaz, Thomas Krieg, Adam Szewczyk, Viacheslav O. Nikolaev, Peter Ruth and Robert Lukowski

*Circulation*. published online October 19, 2017;

*Circulation* is published by the American Heart Association, 7272 Greenville Avenue, Dallas, TX 75231

Copyright © 2017 American Heart Association, Inc. All rights reserved.

Print ISSN: 0009-7322. Online ISSN: 1524-4539

The online version of this article, along with updated information and services, is located on the World Wide Web at:

<http://circ.ahajournals.org/content/early/2017/10/18/CIRCULATIONAHA.117.028723>

Data Supplement (unedited) at:

<http://circ.ahajournals.org/content/suppl/2017/10/18/CIRCULATIONAHA.117.028723.DC1>

**Permissions:** Requests for permissions to reproduce figures, tables, or portions of articles originally published in *Circulation* can be obtained via RightsLink, a service of the Copyright Clearance Center, not the Editorial Office. Once the online version of the published article for which permission is being requested is located, click Request Permissions in the middle column of the Web page under Services. Further information about this process is available in the [Permissions and Rights Question and Answer](#) document.

**Reprints:** Information about reprints can be found online at:

<http://www.lww.com/reprints>

**Subscriptions:** Information about subscribing to *Circulation* is online at:

<http://circ.ahajournals.org/subscriptions/>

## SUPPLEMENTAL MATERIAL

### SUPPLEMENTAL METHODS

#### *Acute open-chest model of ischemia and reperfusion injury*

For studying I/R injury an open-chest, *in situ* model was applied as previously described.<sup>1-3</sup> In brief, mice were anesthetized with pentobarbital-Na<sup>+</sup> (70 mg/kg, *i.p.*). When required, additional *anesthetic* agent was administered as the adequate depth of anesthesia was controlled throughout the surgery. Body temperature was maintained at 37 ± 0.5°C. The animals were ventilated with oxygen by using a mechanical ventilator with a pressure-controlled ventilation mode (peak inspiratory pressure of 10 mbar, positive end-expiratory pressure of 3 mbar). The ventilation frequency was set to 110 breaths/min with a tidal volume of 200-250 µl. The exposure of the heart and thereby of the left coronary artery (LCA) was performed by a left anterior thoracotomy. For induction of ischemia the LCA was surrounded and occluded with a 7-0 polypropylene suture. Successful occlusion was confirmed by an immediate color change of the vessel and cardiac tissue distal to the ligature from red to white. All hearts were subjected to 30 min ischemia followed by 2 hours of reperfusion (I/R; Suppl. Fig. 1, ①). Suppl. Fig. 1 summarizes the details regarding the different treatment protocols applied. Briefly, sham operations were performed as described for the I/R procedure but without occlusion of the LCA (Suppl. Fig. 1, ②). Ischemic postconditioning (iPost; Suppl. Fig. 1, ③) was performed by six consecutive cycles of 10 s reperfusion and 10 s re-occlusion directly after the prolonged index ischemia.<sup>1</sup> For ischemic preconditioning (iPre; Suppl. Fig. 1, ④) 5 min of ischemia followed by 10 min of reperfusion were applied prior to the I/R episode.<sup>2</sup> The BK channel blocker paxilline (PAX, 8 mg/kg in 10% DMSO in H<sub>2</sub>O; Suppl. Fig. 1, ⑤) was administered by *i.p.* injection 5 min after the time of ischemia onset.<sup>4, 5</sup> The BK channel opener NS11021 (9.2 µg/kg in 0.07% DMSO in 0.9% saline, intratrial; Suppl. Fig. 1, ⑥) and riociguat (RIO, 50 ng, *i.v.*; Suppl. Fig. 1, ⑦)<sup>6</sup> were given 5 min before reperfusion. Cinaciguat (CIN, 10 µg/kg in 0.25% DMSO/0.9% saline; Suppl. Fig. 1, ⑧) was injected *i.p.* 30 min before ischemia.<sup>7</sup> Sildenafil (SIL, 2 µg/kg in 0.9% saline; Suppl. Fig. 1, ⑨) was administered 5 min before reperfusion into the left atrium.<sup>1</sup> Tadalafil (TAD, 1 mg/kg in 40% DMSO/H<sub>2</sub>O; Suppl. Fig. 1, ⑩) was given *i.p.* 60 min prior to ischemia.<sup>8</sup> N<sub>w</sub>-nitro-L-arginine methyl ester (L-NAME, 5 mg/ml, Suppl. Fig. 1, ⑪) was provided in the drinking water for 4-5 days before the I/R procedure.

For determination of infarct size a double staining technique with Evans blue and triphenyltetrazolium chloride (TTC) was used.<sup>2</sup> First, the area at risk (AAR) that refers to the tissue, which was affected by the occlusion of the LCA, was determined by retrograde injection of 1% Evans blue dye into the aorta after re-occlusion of the LCA. The heart was then excised and immediately frozen at -20°C. After 20 min the heart was cut into 1-mm slices, which were incubated in 1% TTC solution at 37°C for 20 min. TTC stains the affected but still viable myocardial tissue in red indicating the presence of dehydrogenase enzymes, whereas necrotic tissue that does not contain active oxidation enzymes remains unstained. Heart slices were fixed with 10% formaldehyde for 24 hours. The total area, the AAR and the area of infarction were determined by planimetric measurements. AAR was calculated as a percentage of the entire ventricular area, myocardial damage is defined as infarct size and was expressed as percentage of the risk zone.

### *Chronic closed-chest model of myocardial infarction*

In the chronic I/R model the duration of reperfusion time was extended to 4 weeks, hence the intubated and ventilated mice were allowed to wake up from the anesthesia after the index ischemia was released.<sup>6</sup> In general, the procedure and the surgical interventions were comparable with the open-chest model, though minor changes are described as follows: For induction of the anesthesia a combination of ketamine (100 mg per kg) and xylazine (5 mg per kg) was injected *i.p.*. General anesthesia was maintained with gaseous isoflurane (0.5-2% in oxygen) after endotracheal intubation. The ventilation frequency was adjusted to 140 breaths/min. A small thoracotomy was executed at the third intercostal space without injuring the ribs. Through the small hole in the chest the LCA was occluded for 30 min to induce myocardial infarction. Afterwards the suture was removed and the thoracic incision was closed thoroughly. Mice were monitored until recovery and buprenorphine (0.05 mg/kg) was given subcutaneously prior to the end of surgery and during recovery when necessary.

### *FRET-based CM-specific cGMP measurements in the open chest model*

Transgenic cGMP sensor mice for the measurement of CM-specific cGMP signals by FRET were described earlier.<sup>9</sup> Imaging was performed in red cGES-DE5 transgenic animals subjected to the open-chest model (without I/R). Cinaciguat (CIN, 10 µg/kg in 0.25% DMSO/0.9% saline, *i.p.*; Suppl. Fig. 1) was used to induce CM-specific cGMP signals. For FRET measurement, a self-built imaging system around Leica M165FC (Leica Microsystems GmbH, Wetzlar, Germany) stereomicroscope was used. cGMP sensor was excited with 400 nm LED (pE-100, CoolLED, Andover, UK). Emission light was split into donor and acceptor channels using the DV2 DualView equipped with the 565 dcxr dichroic mirror and D520/30 and D630/50 emission filters (Photometrics, Tucson, AZ, USA). Images were taken using an optiMOS camera (QImaging, Surrey, BC, Canada) with MicroManager 1.4 open source imaging software and analysed by Image J (NIH, USA). Raw data were corrected offline for the bleed-through factor of the donor into the acceptor channel.

### *Blood pressure measurement*

Mean arterial blood pressure (MAP) and heart rate were measured via a telemetry system as previously described (DSI, catheter model TA11PA-C10).<sup>10</sup> For catheterization, mice were anesthetized with isoflurane (0.5-2% in oxygen). Isoflurane levels were adjusted to make surgery tolerable by frequently monitoring the corneal and withdraw reflexes. A ventral midline incision was performed and the left *arteria carotis communis* was carefully dissected. For the ligation two sutures (7-0 resorba silk) were placed about 8 mm apart under the vessel. With the suture proximal to the bifurcation of the left carotid artery the vessel was permanently occluded. The distal suture was used to stretch the vessel in the direction of the aortic arch in order to allow the insertion of the catheter via a tiny incision which was introduced by using a cannula with a right-angle tip. The inserted catheter tip was advanced to the catheter's diminution towards the origin of the carotid artery at the aortic arch and was then permanently fixed by the distal suture and an additional suture placed around the catheterized vessel. The transmitter was positioned in a subcutaneous pocket along the right flank of the animal and then all wounds were closed with 5-0 silk. Measurements were started at day 7 after surgery when mice had fully recovered. Drugs were administered as described in Suppl. Fig. 1. Radiotelemetric signals were recorded for 60 s every 15 min at baseline (48 h) and on day 3 to 5 after starting the L-NAME treatment. For blood pressure (BP) measurements in anesthetized mice, animals were directly placed on a heating plate

after induction of anesthesia by the injection of pentobarbital-Na<sup>+</sup>. Recordings were started 15 min after the respective injection for 10 s every 30 s for a total time of 15 min.

#### *Echocardiographic measurements*

Transthoracic echocardiography was performed using an existing protocol with minor variations.<sup>11</sup> In brief, high-resolution images were acquired by the use of an imaging system equipped with a 30-MHz probe (Vevo2100; VisualSonics, Toronto, ON, Canada). Mice were anesthetized with isoflurane (0.5-2% in oxygen) and placed on a heating plate in a supine position. The chest was gently shaved and cleaned with alcohol to minimize ultrasound reduction. Continual ECG monitoring was obtained via limb electrodes. Two-dimensional echocardiographic study was performed in the parasternal long-axis in three different positions. For determination of heart function under basal conditions, fractional shortening (FS) and ejection fraction (EF) were calculated in M-mode recordings from end-systole and end-diastole measurements in three repeated cardiac cycles of each position permitting us to calculate the mean of 9 values for each parameter.

After myocardial infarction (I<sub>30</sub>/R<sub>4wks</sub>) speckle-tracking based strain analysis of two-dimensional echocardiographic images acquired from the B-mode in parasternal long-axis view was quantified in the longitudinal and radial axes. Strain analysis were conducted by the same trained investigator on all animals according to a previously published protocol<sup>12</sup> using a speckle-tracking algorithm provided by VisualSonics (VevoStrain 2100, VisualSonics). Three consecutive cardiac cycles in the B-mode were selected for analysis based on image quality. Semi-automated tracing of the endocardium and epicardium was performed and corrected as needed. Strain measures were averaged over the obtained cardiac cycles resulting in curvilinear data of strain, strain rate and velocity. Each parameter was divided into 6 segments along the long-axis of the left ventricle (AB: anterior base, AM: anterior mid, AA: anterior apex, PB: posterior base, PM: posterior mid, PA: posterior apex; Suppl. Fig. 10). Peak values were recorded from each of the 6 segments. For global values, measurements were averaged across all 6 segments.

#### *Coronary flow measurements in the Langendorff mouse heart model of I/R*

Animals were deeply anesthetized with isoflurane and anticoagulated by intraperitoneal injection of heparin (1,000 IE/kg). After cervical dislocation, hearts were excised and placed on ice-cold modified Krebs-Henseleit solution (in mmol/L): NaCl (118.0), KCl (4.7), CaCl<sub>2</sub> (2.5), KH<sub>2</sub>PO<sub>4</sub> (1.2), Mg<sub>2</sub>SO<sub>4</sub> (1.2), Na-pyruvate (2.0), NaHCO<sub>3</sub> (25.0), and glucose (11.0) at pH 7.4 – 7.5. The aorta was cannulated, quickly attached to the perfusion system (Hugo Sachs Elektronik/Harvard Aparatus, Germany) and retrograde perfusion was started at a constant pressure of 80 mmHg with continuously warmed (37°C) and aerated (95% O<sub>2</sub>/5% CO<sub>2</sub>) modified Krebs-Henseleit solution. A 2F octapolar electrophysiology catheter with 0.5 mm electrode spacing (CIB'ER Mouse, NuMed Inc., Hopkinton, NY, USA) was inserted into the right atrium and right ventricle for recording of intracardiac electrograms via an ECG amplifier (F104, ADInstruments). Perfusion rate, coronary flow (CF, in milliliters blood per minute per gram myocardium) and heart rate were continuously recorded using a digital data acquisition system and corresponding software (Powerlab8/30 & Labchart, ADInstruments). During the experiments, hearts were kept in an enclosed water-jacketed chamber with ambient temperature maintained at 37°C and were allowed to beat spontaneously.

Control hearts were subjected to 40 min of equilibration, followed by 30 min global zero-flow ischemia and 60 min reperfusion and CF was continuously recorded. An iPre protocol that afforded cardioprotection in the open-chest model of I/R (Suppl. Fig. 1) was applied to hearts

in the Langendorff-perfused iPre group for assessing CF. In detail, iPre hearts were subjected to a 25 min equilibration period, then one cycle of 5 min global zero-flow ischemia and 10 min reperfusion, followed by 30 min global zero-flow ischemia and 60 min reperfusion.

#### *Cardiac troponin I enzyme measurement*

Cardiac troponin I (cTnI) was measured in blood serum of mice at the end of reperfusion. Blood was obtained from the portal vein. After 30 min at 4°C blood samples were centrifuged for 15 min at 4000 rpm at 4°C. cTnI was determined in serum supernatants according to the manufacturer's recommendation of the high sensitivity mouse cTnI ELISA kit (2010-1-HS, Life diagnostics).

#### *Isolation of adult cardiomyocytes*

Adult CMs were isolated as described previously by a modified protocol of the Alliance for Cellular Signaling (AfCS procedure protocol PP00000125).<sup>10, 11, 13</sup> After retrograde enzyme perfusions via the aorta, isolated hearts were minced and cardiomyocytes were liberated by gently applying mechanical turbulence. Quality and purity of the purification was checked visually under the microscope. For hypoxia experiments, Lactate dehydrogenase (LDH) measurements and DNA extraction we used cardiomyocyte cultures with an initial vitality of ≥90%.

#### *Hypoxia treatment of adult cardiomyocytes*

Freshly isolated CMs were resuspended in HEPES-buffered medium (113 mmol/l NaCl, 4.7 mmol/l KCl 4.7, 10 mmol/l HEPES, 1.2 mmol/l MgSO<sub>4</sub>, 30 mmol/l taurine, 1 mmol/l CaCl<sub>2</sub>, 5% bovine calf serum, 5.5 mmol/l glucose, pH 7.4 and 37°C) supplemented with BDM (500 mmol/l). After equilibration, the culture medium was immediately changed and CMs were divided into two groups. For hypoxia, cells were incubated with oxygen-, glucose-, and serum-depleted hypoxia buffer (113 mmol/l NaCl, 4.7 mmol/l KCl 4.7, 10 mmol/l HEPES, 1.2 mmol/l MgSO<sub>4</sub>, 30 mmol/l taurine, 1 mmol/l CaCl<sub>2</sub>, pH 7.4 and 37°C) in an O<sub>2</sub>/CO<sub>2</sub> incubator with an atmosphere of 5%CO<sub>2</sub>/95%N<sub>2</sub> at 37°C for 90 min. For control conditions cells were incubated in normal HEPES-buffered medium in an atmosphere of 21% O<sub>2</sub> and 5% CO<sub>2</sub> at 37°C for 90 min.

#### *Lactate dehydrogenase measurements in CM cultures*

LDH activity was detected using CytoTox 96 NonRadioactive Cytotoxicity kit (Promega, G1780). After normoxia/hypoxia, the medium was collected by centrifugation and LDH release was measured according to the manufacturer's instructions. Protein content was determined by Bradford method for normalizing the LDH data.

#### *Purification of cardiomyocyte mitochondria*

Mitochondria from adult cardiomyocytes were isolated according to a protocol published by Frezza and co-workers.<sup>14</sup> In brief, after perfusion of the heart and mechanically liberation of cells, CMs were centrifuged and homogenized using a glass-teflon potter in IBm1 buffer (50 mmol/l Tris-HCl, 10mmol/l EDTA/Tris, 67 mmol/l sucrose, 50 mM KCl, 0,2% BSA, pH 7.4) at 4°C. Subsequently, the mitochondrial fraction was separated by three centrifugation steps at 700 g and 8000 g at 4°C for 10 min each. The resulting cell pellet was finally resuspended in IBm2 buffer (10 mmol/l Tris-HCl, 250 mmol/l sucrose, 3 mmol/l EGTA, pH 7.4), centrifuged again at 8000 g at 4°C for 10 min and then resuspended in a final volume of 30 µl SDS

protein lysis buffer. The postmitochondrial supernatant served as the source for the cytosolic fraction, which was further centrifuged at 100,000 g for 1 h in a ultracentrifuge to ensure complete clearance of mitochondrial fragments. The cytosolic proteins were precipitated by adding 1/10 volume of 100% TCA, and the proteins were collected by centrifugation at 14,000 rpm at 4°C for 10 min. After washing three times with ice-cold 80% acetone, the pellet was suspended in SDS protein lysis buffer. Western Blot analyses were performed only with fresh isolated mitochondria or cytosolic fractions directly after the purification as described below.

#### *Measurement of mitochondrial respiration*

Oxygen consumption of cardiomyocyte mitochondria was measured polarographically at 37°C using a Clark-type electrode in a medium containing 250 mM sucrose, 10 mM Tris-HCl, 5 mM MgCl<sub>2</sub>, 2 mM KH<sub>2</sub>PO<sub>4</sub>, and 20 μM EGTA, pH 7.4. Mitochondria (0.3 mg/ml as protein) were suspended in 1 ml of the respiration medium. After a stable baseline, state 2 respiration was initiated by addition of 5 mM glutamate/ 2.5 mM malate or 5 mM succinate. State 3 respiration was initiated by addition of 100 μM ADP. State 4 refers to the respiration when all the added ADP is converted to ATP.

#### *Patch-clamp experiments on isolated cardiomyocyte mitoplasts*

Patch-clamp experiments using mitoplasts were performed as described previously.<sup>15, 16</sup> Briefly, mitoplasts were prepared from BK<sup>+/+</sup> and BK<sup>-/-</sup> cardiomyocyte mitochondria placed in a hypotonic solution (5 mM HEPES, 100 μM CaCl<sub>2</sub>, pH 7.2) for approximately 5 min to induce swelling and breakage of the outer membrane. To restore the isotonicity, a hypertonic solution (750 mM KCl, 30 mM HEPES, 100 μM CaCl<sub>2</sub>, pH 7.2) was added to the medium. The patch-clamp pipette was filled with an isotonic solution containing 150 mM KCl, 10 mM HEPES, and 100 μM CaCl<sub>2</sub> at pH 7.2. Mitoplasts were easily distinguished from other cellular debris by their size, round shape, transparency, and the presence of a “cap” structure. An isotonic solution containing 100 μM CaCl<sub>2</sub> was used as the control solution for all experiments. The low calcium solution (1 μM CaCl<sub>2</sub>) contained 150 mM KCl, 10 mM HEPES, 1 mM EGTA and 0.752 mM CaCl<sub>2</sub> at pH = 7.2. All test compounds were added to the isotonic solution containing 100 μM CaCl<sub>2</sub> by applying a perfusion system containing a custom-made holder with a glass tube, a peristaltic pump, and Teflon tubing. The mitoplast membranes at the tip of the measuring pipette were transferred into the opening of the multibarrel “sewer pipe” system where they were rinsed with the test solutions (inside-out configuration) (see Suppl. Fig. 15 for further details). Reported voltages are those applied to the patch-clamp pipette interior. Hence, positive potentials represent the physiological polarization of the inner mitochondrial membrane (outside positive). The electrical connection was made using Ag/AgCl electrodes and an agar salt bridge (3 M KCl) as the ground electrode. Current was recorded using a patch-clamp amplifier (Axopatch 200B, Molecular Devices Corporation, USA). The pipettes, made of borosilicate glass, had a resistance of 10-20 MΩ and were pulled using a Narashige P-10 puller.

The currents were low-pass filtered at 1 kHz and sampled at a frequency of 100 kHz. The traces of the experiments were recorded in single-channel mode. The illustrated channel recordings are representative of the most frequently observed conductance for the given condition. The conductance of the channel was calculated from the current-voltage relationship (Fig. 7B). The probability of channel opening (P<sub>o</sub>, open probability) was determined using the single-channel search mode of the Clampfit 10.7 software.

*Measurement of mitochondrial hydrogen peroxide in vivo*

Mitochondrial hydrogen peroxide was determined *in vivo* using the MitoB mass spectrometric probe.<sup>17, 18</sup> MitoB (50  $\mu$ l/0.5 mM) was administered by tail-vein injection 60 min prior to I/R. After 30 min ischemia, followed by 120 min reperfusion 53.0  $\pm$  2.0 mg of the suspected ischemic heart area was visually identified, dissected, frozen on liquid nitrogen and stored at -80°C. Accordingly, normoxic tissue was collected from sham-operated mice injected with MitoB. For analysis, the homogenized tissue was spiked with deuterated internal standard. MitoB and its product MitoP (from the reaction with hydrogen peroxide) were extracted and the amounts MitoB and MitoP in the ischemic tissue were determined by liquid chromatography and tandem mass spectrometry as previously described.<sup>17</sup>

*Preparation of cryosections*

Hearts, and for particular tests aorta, were excised from experimental mice and directly fixed in 4% paraformaldehyde. Using a sucrose gradient, tissues were dehydrated and preserved in embedding medium for storage at -80°C. Cryosections of 10  $\mu$ m were prepared using a Microm HM microtome (Thermo Scientific). Each heart was separated into 8 equidistant regions from the apex to the ligation and for each region 3 consecutive 10- $\mu$ m sections were analyzed by TUNEL and hematoxylin & eosin (H&E) staining (Fig. 4E).

*TUNEL, H&E, Sirius red and PermaFluor/Hoechst stainings*

Myocardial cell death by apoptosis was detected in cryosections using a commercial TUNEL kit according to the manufacturer's recommendations (Merck Millipore, S7101).

To visualize histological structures, cardiac sections from different regions distal to the ligature were rehydrated and then stained using hematoxylin and eosin (*H&E*). Sections were incubated for 5 s in hematoxylin solution after Harris, followed by 2 washings steps and differentiation of the blue color in 0.1% ammonia solution before acidic eosin Y solution was added as a *cytoplasmic* counterstain for 10 min. For color differentiation cardiac sections were incubated in ethanol (80-100%) followed by a dehydration using toluol.

To study the amount of fibrosis after myocardial infarction, hearts from CMBK-KO and -CTR mice which were subjected to the chronic model of MI were dissected, cut into 8 equidistant regions and *cryosectioned*. Before adding Sirius red staining solution (0.1% Direct Red 80 dissolved in aqueous saturated picric acid) for 1 h representative 10- $\mu$ m sections from each heart region were fixed in Bouin solution (HT101126, Sigma-Aldrich) for 24 h at room temperature. After several washing steps to remove excess dye in 0.01 N HCl, the samples were dehydrated using a gradient of ethanol (50% to 100% in steps of 10%) and xylol (100%). H&E and Sirius red sections were finally mounted in in DePeX and analyzed using an Axiovert 200M microscope (Zeiss).

Nuclei in cryosections of hearts and aortas from  $\alpha$ MHC-Cre transgenic ROSA26-tomato reporter mice were visualized by 0.1% Hoechst in PermaFluor aqueous mounting media (TA-030-FM, Thermo Fisher Scientific) using a fluorescent ApoTome microscope (Zeiss). Recombination efficacy was assessed by quantifying the switch from cell membrane-localized red fluorescence (mT) to membrane-localized green fluorescence (mG) protein.



*Western blot analysis*

Hearts obtained from CMBK-KO and -CTR mice were excised under basal conditions or after 30 min of ischemia followed by either 10 min (I<sub>30</sub>/R<sub>10</sub>) or 120 min (I/R) of reperfusion. The ischemic part distal to the ligation was immediately homogenized in 400 µl SDS lysis buffer (2.1% Tris-HCl (1 M), pH 8.3; 0.67% SDS; 1.7% β-mercaptoethanol; 0.2% phenylmethylsulfonyl fluoride; 1% phosphatase inhibitor cocktails 2 and 3 (Sigma-Aldrich) in dH<sub>2</sub>O) using a homogenisator for 90 s followed by 1 min centrifugation at 1500 rpm. Supernatants were denaturated for 10 min at 95°C and stored at -80°C until further analysis. After protein quantification gels were loaded with 75 µg total protein or 4 µl of a molecular-weight size marker (prestained protein marker IV, Peqlab) in 16 µl dH<sub>2</sub>O per line. Separation of proteins by molecular weight was done by SDS-Polyacrylamide gel electrophoresis (PAGE). Transfer of proteins that have been separated by *SDS-PAGE* to a polyvinylidene difluoride (PVDF) membrane was carried out by using a semi-dry transfer system. For immunodetection primary BK $\alpha$ (674-1115) (1:500 dilution, custom-made)<sup>19, 20</sup>, BK $\alpha$ (690-1196) (1:1000 dilution, NeuroMab clone L6/60), cGKI $_{\alpha/\beta}$  (1:500 dilution, generous gift from Prof. Franz Hofmann, TU München), cGKI $_{CST}$  (1:1000 dilution, Cell Signaling Technology, #3248), manganese superoxide dismutase (MnSOD, 1:2000 dilution, Enzo Life Science, ADISOD110J), copper-zinc superoxide dismutase (CuZnSOD, 1:2000 dilution, Enzo Life Science, ADISOD101J), TOM20 (1:100 dilution, Santa Cruz, sc-17764), hsp60 (1:200 dilution, Santa Cruz, sc13966), cytochrome C (Cyt C, 1:1000 dilution, Cell Signaling Technology, #11940), Complex I (1:1000 dilution, proteintech, 12444-1-AP), β1-AR (1:200 dilution, Santa Cruz, sc-568), COX IV (1:1000 dilution, Cell Signaling Technology, #4844), GAPDH (1:1000 dilution, Cell Signaling Technology, #2118), α-tubulin (1:1000 dilution, Cell Signaling Technology, #3873), p44/42 MAPK (ERK, 1:1000 dilution, Cell Signaling, #9102), phospho-p44/42 MAPK (p-ERK, 1:1000 dilution, Cell Signaling, #9101), Akt (1:1000 dilution, Cell Signaling, #9272), phospho-Akt (1:1000 dilution, Cell Signaling, #4060), vasodilator-stimulated phosphoprotein (VASP, 1:1000 dilution, Cell Signaling, #3132), and phospho-VASP (1:500 dilution, Enzo Life Science, ALX804240C100) antibodies were used. Anti-mouse secondary antibodies coupled to Cy3 (PA43009) or anti-rabbit secondary antibodies coupled to Cy5 (PA40511) were used in a 1:2500 dilution (GE Healthcare) to detect the formation of primary *antibody-antigen complexes*. To quantify the amount of fluorescence an *Ettan DIGE* Imager or Amersham Imager 600 system (GE Healthcare) was used to produce multichannel images of the Western Blots.

**SUPPLEMENTAL TABLES**

**Suppl. Tab. 1** *Baseline characteristics of CMBK-CTR and -KO mice*

		BW [g]	HW [mg]	TL [mm]	HW / BW [mg/g]	HW / TL [mg/mm]
♂	CMBK <sup>+fl</sup> (n=7)	24.9 ± 0.4	117.3 ± 2.8	16.91 ± 0.20	4.71 ± 0.07	6.93 ± 0.13
	CMBK <sup>-fl</sup> (n=9)	24.5 ± 0.7	116.3 ± 3.0	16.79 ± 0.17	4.75 ± 0.11	6.92 ± 0.13
♀	CMBK <sup>+fl</sup> (n=6)	22.4 ± 0.6	94.2 ± 2.8	16.63 ± 0.14	4.22 ± 0.11	5.66 ± 0.15
	CMBK <sup>-fl</sup> (n=6)	22.0 ± 0.6	97.1 ± 3.3	16.72 ± 0.26	4.41 ± 0.08	5.81 ± 0.15

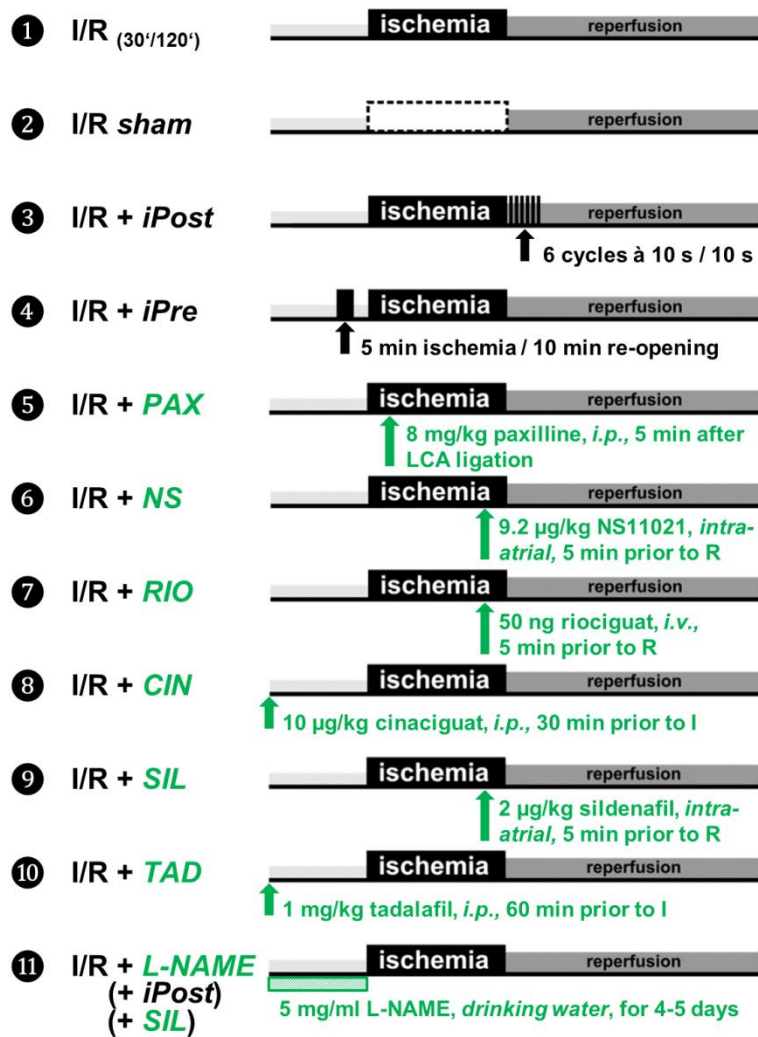
Lack of CM-specific BK channels did neither affect heart weight (HW), body weight (BW) or tibia length (TL), nor the respective HW/BW and HW/TL ratios calculated from these values.

**Suppl. Tab. 2** Significant increase in heart weight parameters after I/R<sub>4wks</sub>

	BW [g]	HW [mg]	TL [mm]	HW / BW [mg/g]	HW / TL [mg/mm]
♂ CMBK <sup>+fl</sup> (n=13)	25.2 ± 0.3	125.3 ± 2.4*	17.27 ± 0.12	4.96 ± 0.07**	7.26 ± 0.14
♂ CMBK <sup>-fl</sup> (n=13)	25.1 ± 0.3	124.6 ± 1.9*	17.31 ± 0.16	4.97 ± 0.05*	7.21 ± 0.12

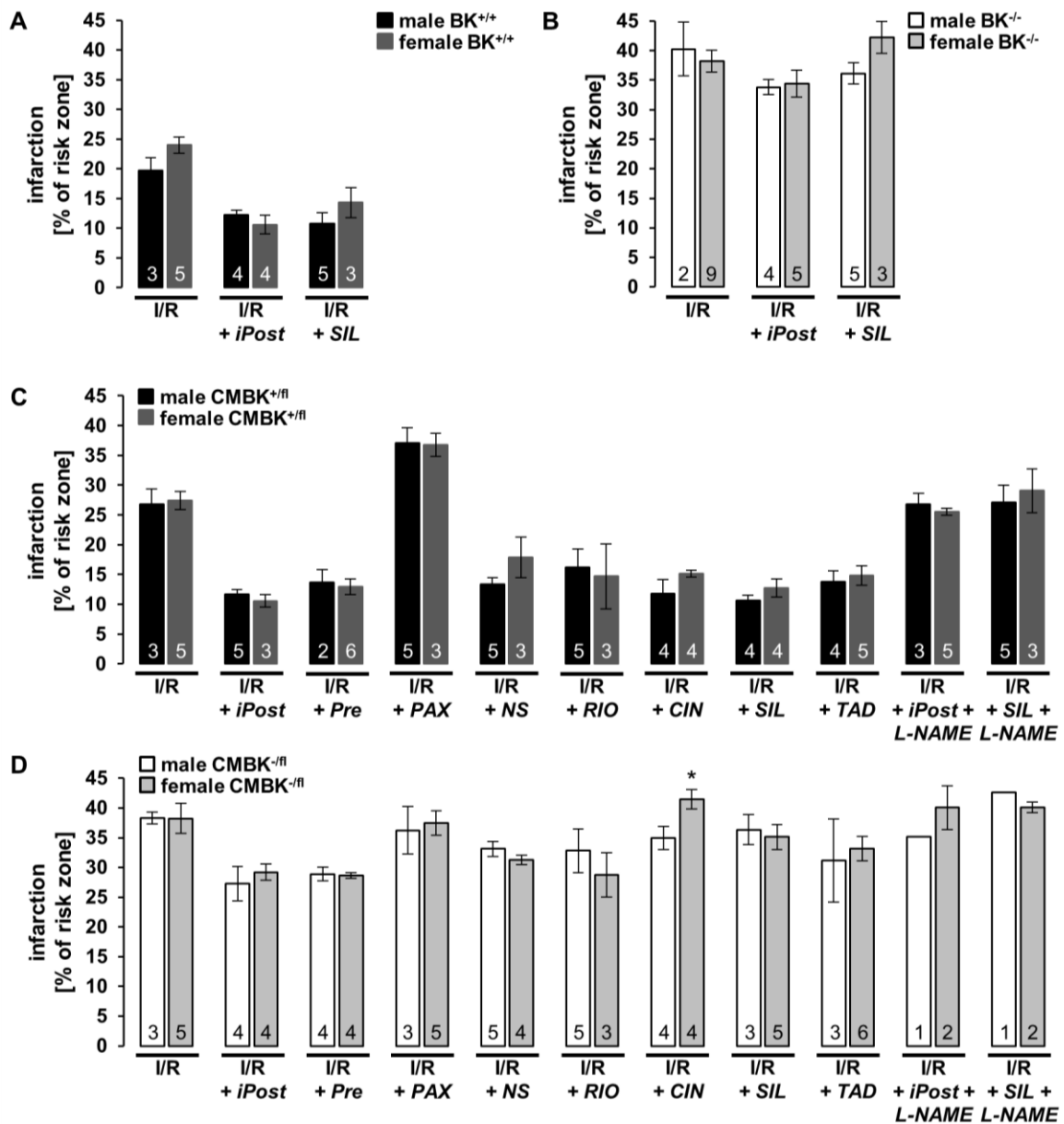
Heart weight was increased after 30 min ischemia followed by 4 weeks reperfusion (I/R<sub>4wks</sub>) independent of the presence or absence of BK in CMs. Data were analyzed using the Student's t-test with \*p<0.05, \*\*p<0.01 basal vs. I/R<sub>4wks</sub> of respective genotype.

SUPPLEMENTAL FIGURES AND FIGURE LEGENDS



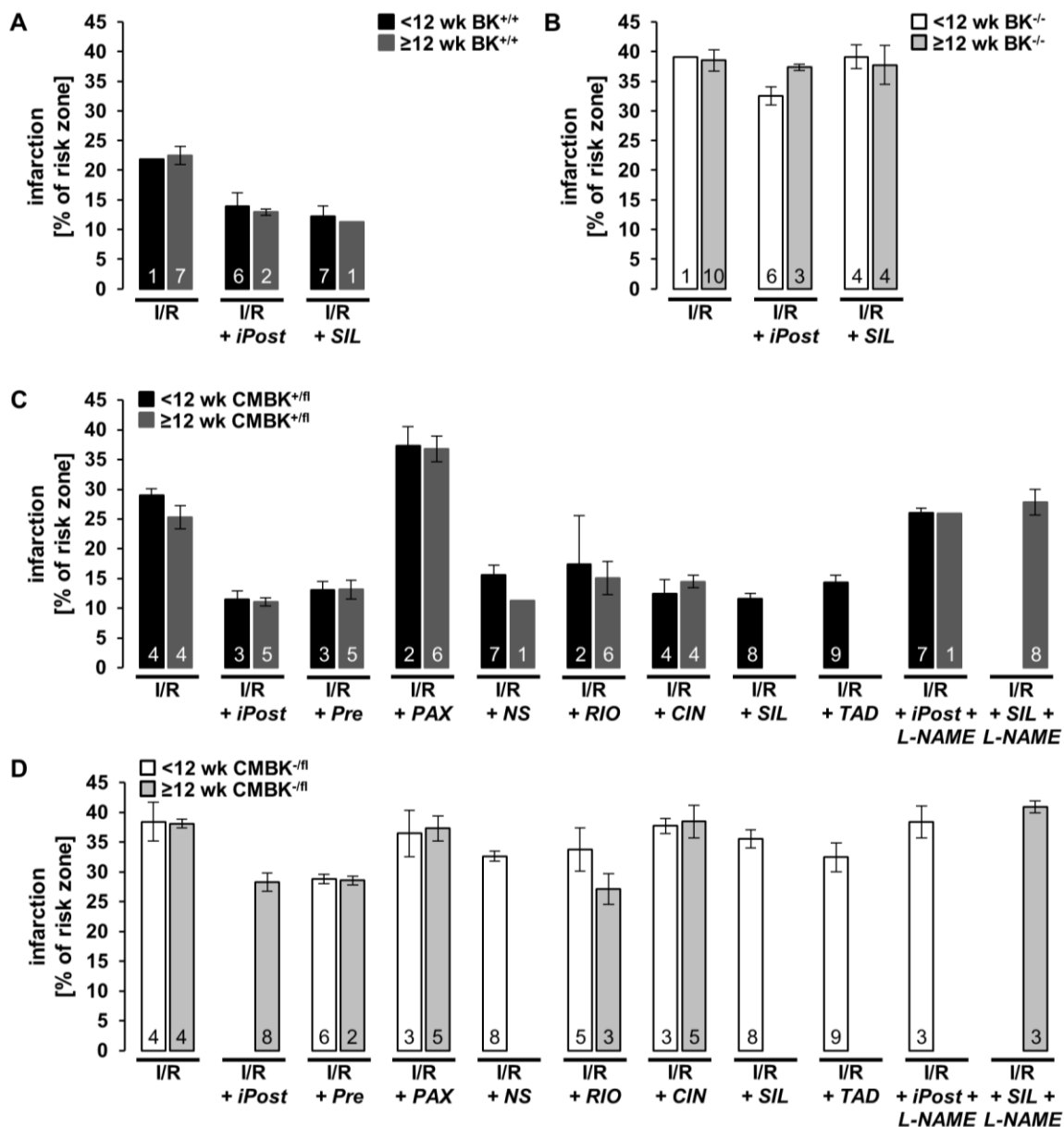
**Suppl. Fig. 1:** Pharmacological treatments and ischemic conditioning procedures in the acute model of myocardial infarction

I/R: 30 min ischemia followed by 120 min reperfusion; *sham*: sham-operated; *iPost*: postconditioning; *iPre*: preconditioning; *PAX*: paxilline; *NS*: NS11021; *RIO*: riociguat; *CIN*: cinaciguat; *SIL*: sildenafil; *TAD*: tadalafil; *L-NAME*: N<sub>ω</sub>-nitro-L-arginine methyl ester



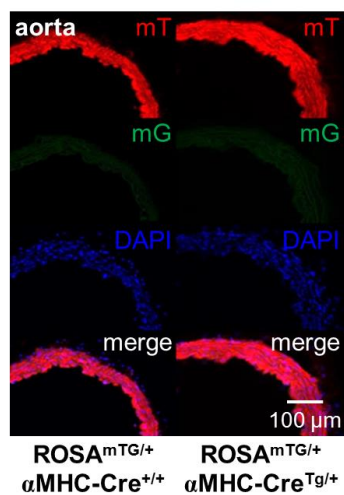
**Suppl. Fig. 2: Sex differences do not influence infarct size**

Overall no gender-specific effects on the infarct size after I/R ( $\pm$  different cGMP-elevating compounds or conditioning protocols) were observed in (A) global BK-WT (BK<sup>+/+</sup>), (B) global BK-KO (BK<sup>-/-</sup>), (C) CMBK-CTR (CMBK<sup>+/fl</sup>) or (D) CMBK-KO (CMBK<sup>-/fl</sup>) mice. In the I/R + CIN treatment group the data just meet the significance criterion ( $p=0.044$ ). *iPost*: postconditioning; *iPre*: preconditioning; *PAX*: paxilline; *NS*: NS11021; *RIO*: riociguat; *CIN*: cinaciguat; *SIL*: sildenafil; *TAD*: tadalafil; *L-NAME*: N<sub>ω</sub>-nitro-L-arginine methyl ester. Data were examined using the Student's t-test with \* $p<0.05$  male vs. female for each setup.



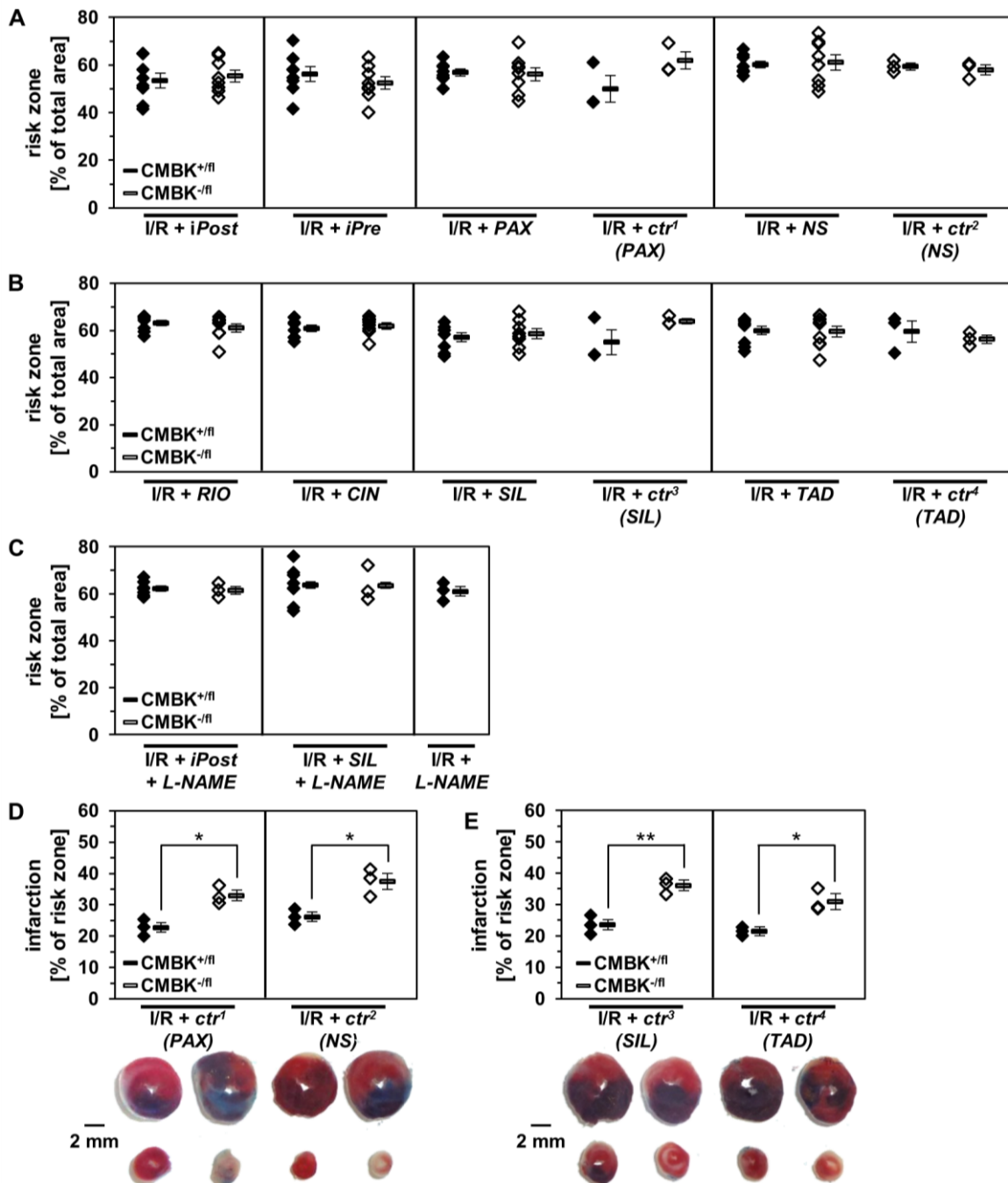
**Suppl. Fig. 3: Infarct size did not depend on age**

Infarct sizes of (A) global BK-WT (BK<sup>+/+</sup>), (B) global BK-KO (BK<sup>-/-</sup>), (C) CMBK-CTR (CMBK<sup>+fl</sup>) or (D) CMBK-KO (CMBK<sup>-fl</sup>) did not differ between mice aged 8 to 11 or 12 to 16 weeks. For the comparison of the MI outcome between KO and control mice littermates or animals at the same age were routinely subjected to one specific I/R setup. *iPost*: postconditioning; *iPre*: preconditioning; *PAX*: paxilline; *NS*: NS11021; *RIO*: riociguat; *CIN*: cinaciguat; *SIL*: sildenafil; *TAD*: tadalafil; *L-NAME*: N<sub>ω</sub>-nitro-L-arginine methyl ester. Data were examined using the Student's t-test with \*p<0.05 <12 weeks vs. ≥12 weeks for each setup.



**Suppl. Fig. 4:** *αMHC-Cre* activity is not detectable in aortic smooth muscle cells

Cell membrane-localized red fluorescence (mT) and membrane-localized green fluorescence (mG) protein were visualized in  $\alpha$ MHC-Cre recombinase positive ( $\alpha$ MHC-Cre<sup>Tg/+</sup>) and Cre-negative ( $\alpha$ MHC-Cre<sup>+/+</sup>) mice that were transgenic for a global double-fluorescent Cre reporter (ROSA<sup>mTG/+</sup>). As expected, mT (red) was expressed in the  $\alpha$ MHC-Cre<sup>+/+</sup>; ROSA<sup>mTG/+</sup> aorta, whereas mG (green) was not detectable. Similarly, no Cre-mediated conversion of the floxed mT to the mG reporter was observed in aortic smooth muscle cells of  $\alpha$ MHC-Cre<sup>Tg/+</sup>; ROSA<sup>mTG/+</sup> mice. DAPI was used as a nuclear counterstain.



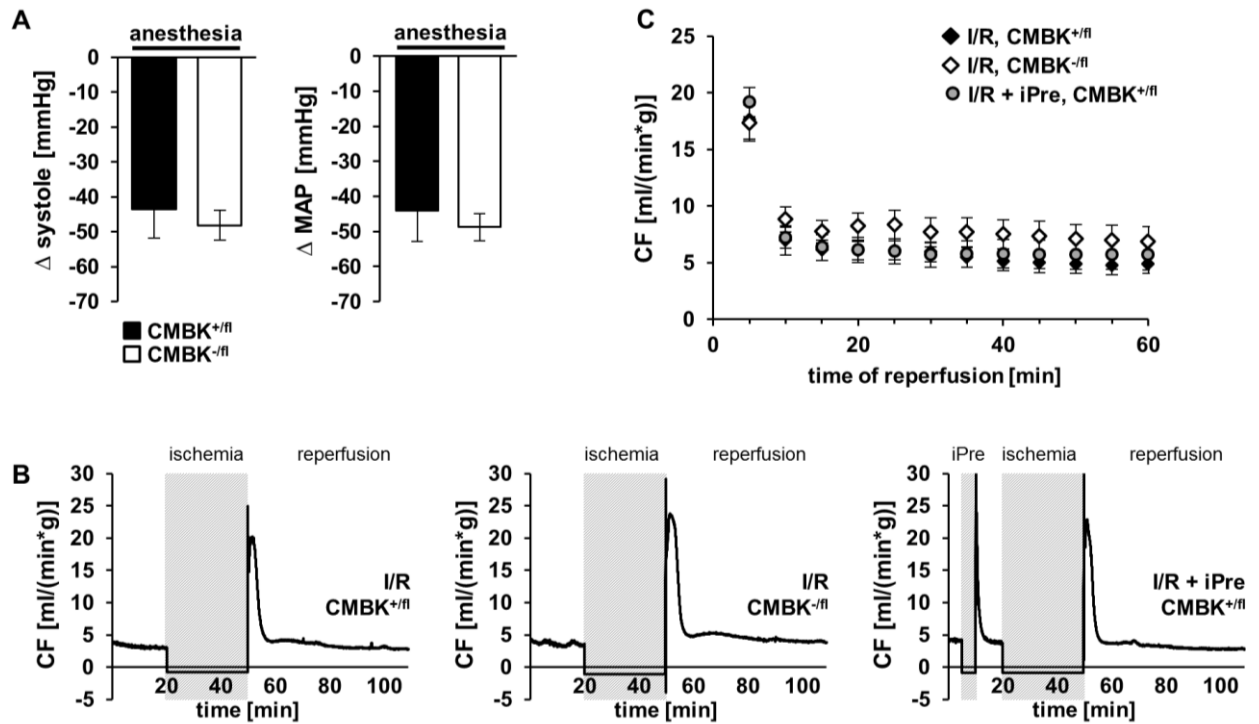
**Suppl. Fig. 5:** Risk zones do not differ between CMBK-CTR and -KO mice and setups

(A) No differences in the area at risk (in %) were observed between the different mechanical interventions and pharmacological treatment regimens that directly modulate BK. (B) Risk zones were comparable between all genotypes and setups using (B) different cGMP-elevating compounds (C) in addition to the NOS-inhibitor L-NAME. (D+E). Administration of a number of solvents did not influence infarct size as compared to I/R. Representative heart slices of the respective genotype and setup (blue: unaffected heart muscle; red plus white: risk zone; white: infarcted tissue) are shown in the lower panel. *iPost*: postconditioning; *iPre*: preconditioning; PAX: paxilline; NS: NS11021; RIO: riociguat; CIN: cinaciguat; SIL: sildenafil; TAD: tadalafil; L-NAME: N<sub>ω</sub>-nitro-L-arginine methyl ester; *ctr*<sup>1</sup> (PAX): 10% DMSO/H<sub>2</sub>O; *ctr*<sup>2</sup>



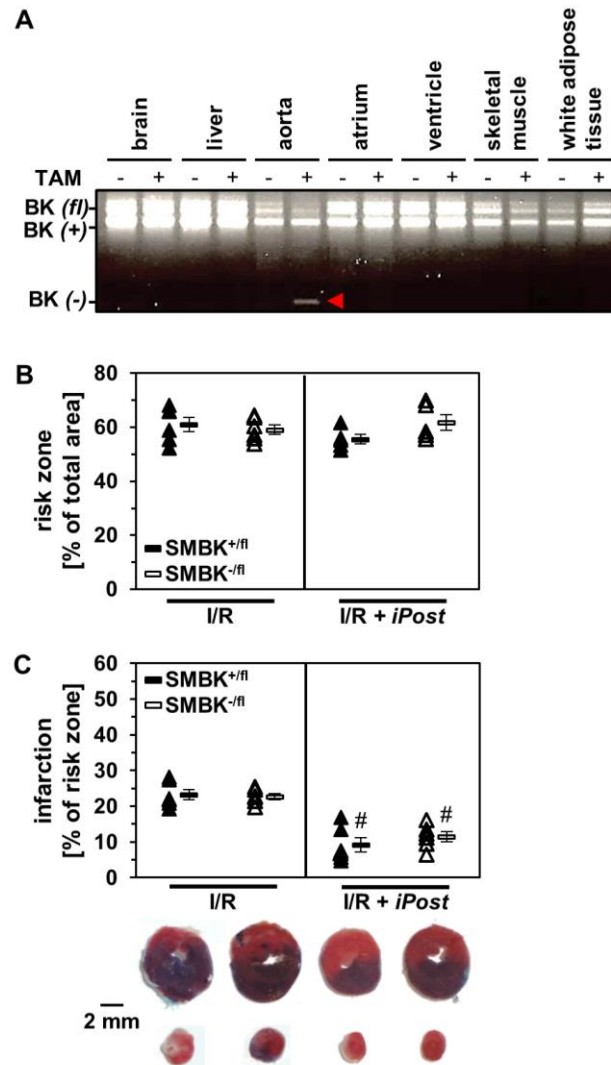
**SUPPLEMENTAL MATERIAL** Frankenreiter *et al.*: Cardiomyocyte-specific BK channels in I/R injury

(NS): 0.07% DMSO/0.9% saline; *ctr*<sup>3</sup> (SIL): 0.9% saline; *ctr*<sup>4</sup> (TAD): 40% DMSO/H<sub>2</sub>O. Data were examined using two-way ANOVA followed by Bonferroni-corrected Student's t-tests with \* $p < 0.05$ , \*\* $p < 0.01$  CMBK<sup>-fl</sup> vs. CMBK<sup>+fl</sup>.



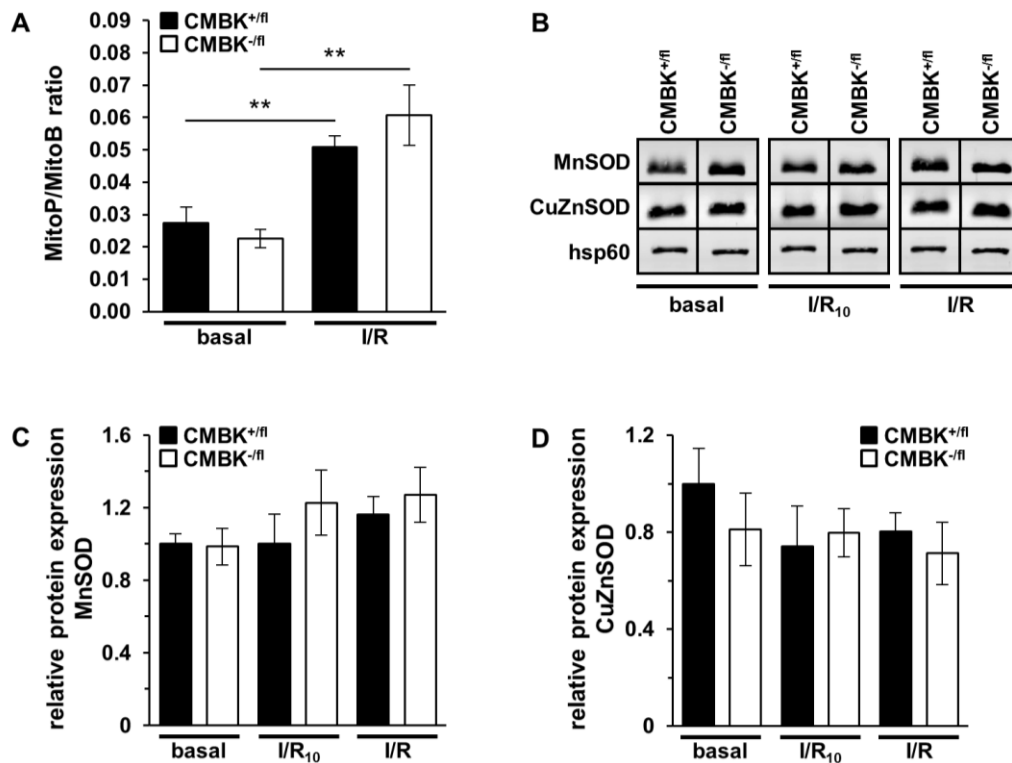
**Suppl. Fig. 6:** Blood pressure during anesthesia and coronary flow are independent of CMBK

(A) Blood pressure drop by anesthesia induced using pentobarbital- $\text{Na}^+$ . Data are means  $\pm$  SEM with  $n=5$  for CMBK<sup>+fl</sup> and  $n=6$  for CMBK<sup>-fl</sup>. (B) Representative traces of coronary flow determined *ex vivo* in Langendorff-perfused heart preparations during I/R with (right panel) and without (left and middle panel) iPre stimulation. (C) Neither the CM-specific deletion of BK nor a preconditioning protocol affording cardioprotection *in vivo* (s. Fig. 5A right panel) significantly affected the coronary flow (CF) at reperfusion ( $n=5$  for each data point). Data analysis using Student's t-test (A) or repeated measures ANOVA (C) did not show statistical significances.



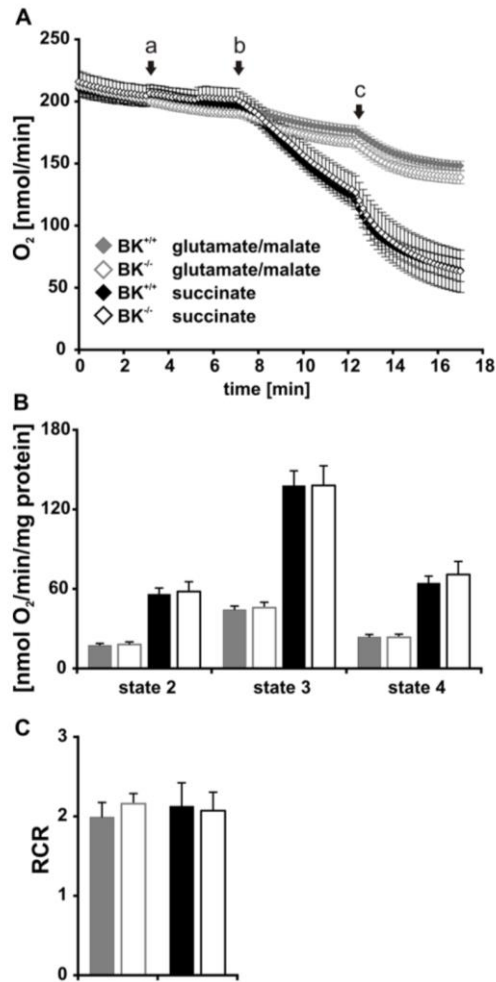
**Suppl. Fig. 7: Smooth muscle cell-specific BK-deficiency does not affect I/R-induced infarct formation**

(A) Genomic PCR analysis of various tissues derived from SMMHC-CreERT2<sup>Tg/+</sup>; BK<sup>+/fl</sup> (SMBK<sup>+/fl</sup>) mice revealed selective recombination of the floxed (*fl*) BK allele to the BK knock-out (-) allele in smooth muscle tissues. The PCR products were amplified by BK-specific primers which allowed co-identification of the (*fl*), (-) and wild-type (+) alleles. (B) Risk zones expressed as percentage of the total heart area after I/R and I/R + *iPost* in smooth muscle cell-specific BK channel mutants (SMBK<sup>-/fl</sup>) and their litter-matched controls (SMBK<sup>+/fl</sup>). (C) Infarction did not differ between SMBK-deficient and SMBK-proficient mice (n=6 per genotype and setup). Representative heart slices of the respective genotype and setup are shown in the lower panel. All data were assessed using two-way ANOVA followed by Bonferroni-corrected Student's t-tests with #: p<0.001 to respective I/R group.



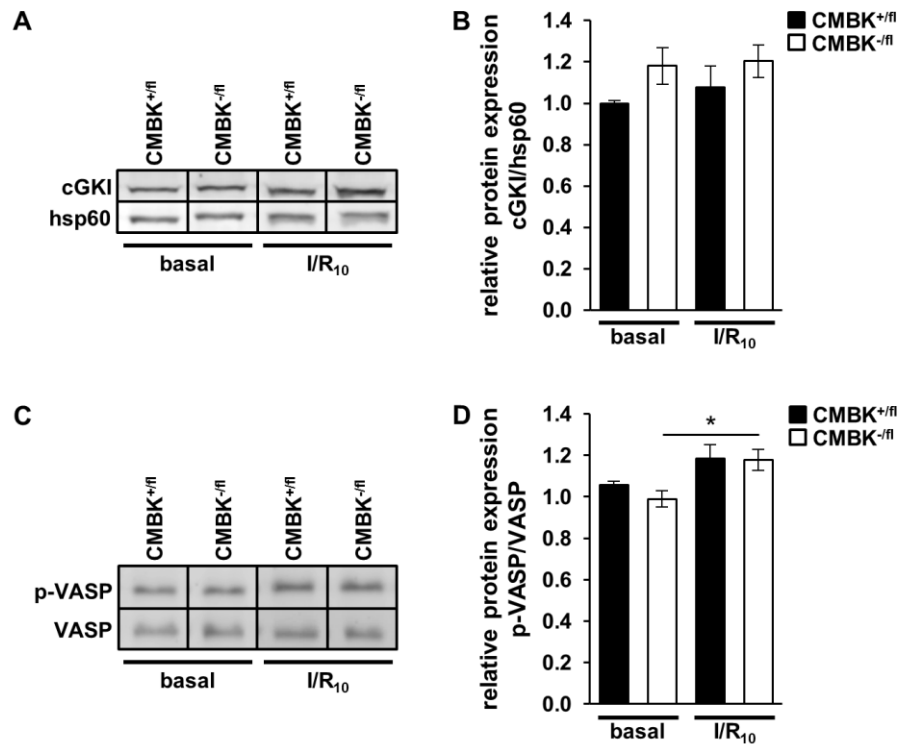
**Suppl. Fig. 8:** Superoxide dismutase expression levels are not modulated by BK during myocardial infarction

(A) The MitoP/MitoB ratio was used as a marker for hydrogen peroxide formation in CMBK-KO (CMBK<sup>-fl</sup>) and -CTR (CMBK<sup>+fl</sup>) hearts at baseline (n=6 per genotype) and after I/R (n=8 per genotype). Mean values at baseline and I/R between genotypes trended towards being different, but this trend did not reach statistical significance. (B) Representative immunoblots showing comparable expression of manganese-dependent superoxide dismutase (MnSOD) and copper/zinc superoxide dismutase (CuZnSOD) at baseline and during myocardial infarction (30 min ischemia / 10 min reperfusion (I/R<sub>10</sub>) and 30 min ischemia / 120 min reperfusion (I/R)) in CMBK-KO (CMBK<sup>-fl</sup>) and -CTR (CMBK<sup>+fl</sup>) hearts. Heat shock protein 60 (hsp60) was co-identified in the protein samples as a loading control. Western blot analysis of the expression of (C) MnSOD and (D) CuZnSOD with n=6 per genotype. Data in (A), (C) and (D) are means ± SEM. Data were analyzed using two-way ANOVA followed by Bonferroni-corrected Student's t-tests with \*\*p<0.01 basal vs. I/R.



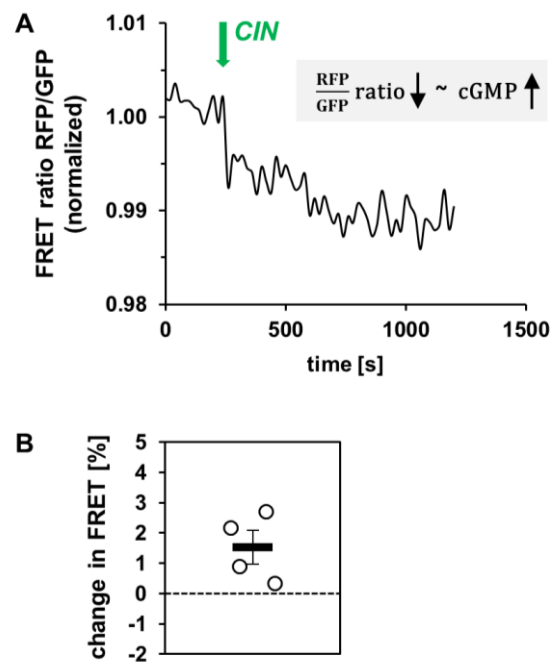
**Suppl. Fig. 9:** *Respiration of cardiomyocyte mitochondria at normoxia*

(A) Traces of mitochondrial respiration from BK-WT (BK<sup>+/+</sup>) and BK-KO (BK<sup>-/-</sup>) cardiomyocyte mitochondria (CMM). After addition of mitochondria (a) state 2 respiration was initiated by addition of glutamate/malate or succinate (b). State 3 respiration (c) was initiated by addition of ADP. (B) Ratios of respiration in the different states did not differ between the two genotypes. (C) Respiratory control ratio (RCR) also showed no differences between BK-WT and BK-KO CMM. Data are mean  $\pm$  SEM with BK<sup>+/+</sup> n=12 for glutamate/malate and n=10 for succinate and BK<sup>-/-</sup> n=11 for glutamate/malate and n=9 for succinate.



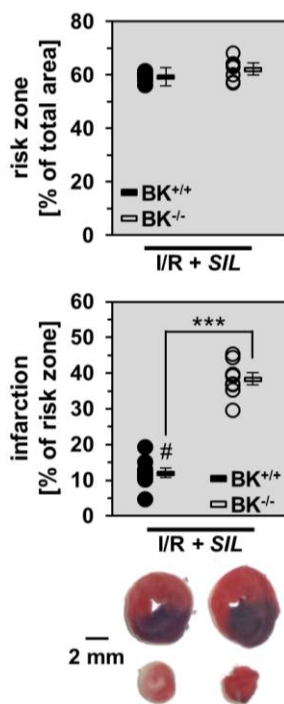
**Suppl. Fig. 10:** Expression of cGKI in CM-specific BK mutant hearts is not altered by myocardial infarction

(A) Representative immunoblots and (B) quantification of the cGKI protein in CMBK-KO (CMBK<sup>-fl</sup>) and -CTR (CMBK<sup>+fl</sup>) heart samples at baseline and during myocardial infarction (30 min ischemia / 10 min reperfusion (I/R<sub>10</sub>)). Heat shock protein 60 (hsp60) was used as loading control. (C) Representative blots and (D) quantification of the vasodilator-stimulated phosphoprotein (VASP) and VASP phosphorylation (p-VASP) at Ser239. Data are means  $\pm$  SEM with n=4 per genotype. Data in (B) were assessed using the Kruskal-Wallis-test. For (D) levels of significance were tested using two-way ANOVA followed by Bonferroni-corrected Student's t-tests with \*p<0.05 basal vs. I/R<sub>10</sub>.



**Suppl. Fig. 11:** *Cinaciguat causes an increase in CM cGMP in vivo*

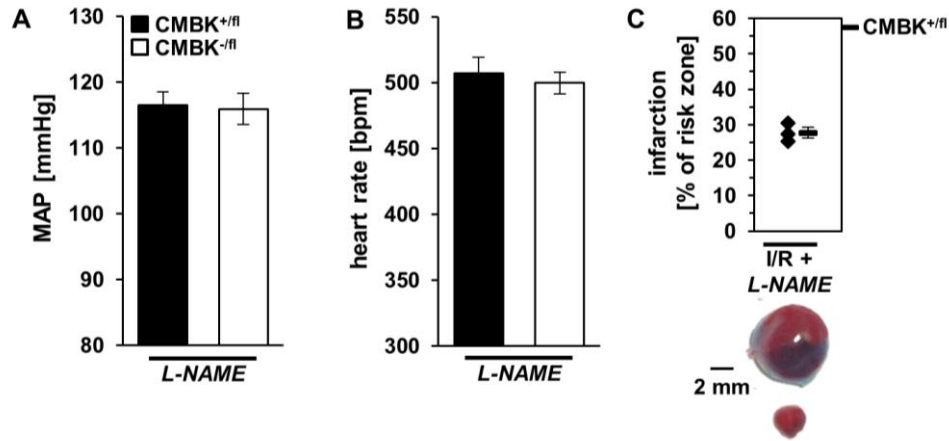
CM-specific cGMP levels were measured in red-cGES-DE5 FRET sensor mice (s. supplemental methods for further details) in the in situ open-chest model. (A) Representative trace showing a decrease in the CM-specific FRET signal indicating an increase in cGMP by cinaciguat (CIN). (B) Overall change in FRET signal 30 min after the cinaciguat challenge. Dots are individual experiments while the bar represents mean  $\pm$  SEM (n=4).



**Suppl. Fig. 12:** *Cardioprotection by sildenafil requires the BK channel*

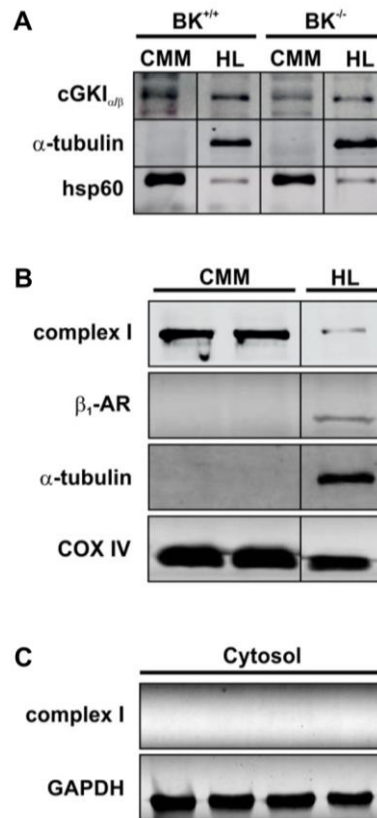
(A) Risk zones and (B) infarct size of global BK-KO (BK<sup>-/-</sup>) hearts  $\pm$  sildenafil. Mice globally lacking BK did not respond to the cardioprotection stimulated by sildenafil. Infarction is expressed as percentage of the risk zone with  $n=8$  per genotype. Representative heart slices of the respective genotype are shown in the lower panel. Data were examined using the Student's t-test with \*\*\* $p<0.001$  BK<sup>-/-</sup> vs. BK<sup>+/+</sup>; #:  $p<0.001$  to respective I/R group.





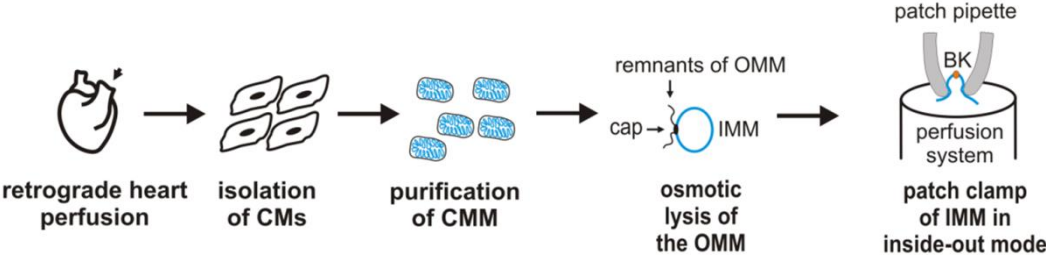
**Suppl. Fig. 13:** Effects of L-NAME on blood pressure in CMBK-CTR and CMBK-KO mice

Administration of the NO synthase inhibitor N<sub>ω</sub>-nitro-L-arginine methyl ester (L-NAME, 5 mg/ml in the drinking water) caused an increase in (A) mean arterial blood pressure (MAP) and (B) a concomitant decrease in heart rate in both genotypes (n=5 per genotype). (C) L-NAME did not affect the infarct size of CMBK-CTR mice (CMBK<sup>+fl</sup>, n=3) subjected to the I/R injury (compared to the respective values shown in Fig. 4B). Infarction is expressed as percentage of the risk zone. (A-B) Student's t-test did not reveal significant differences between genotypes (p<0.05).

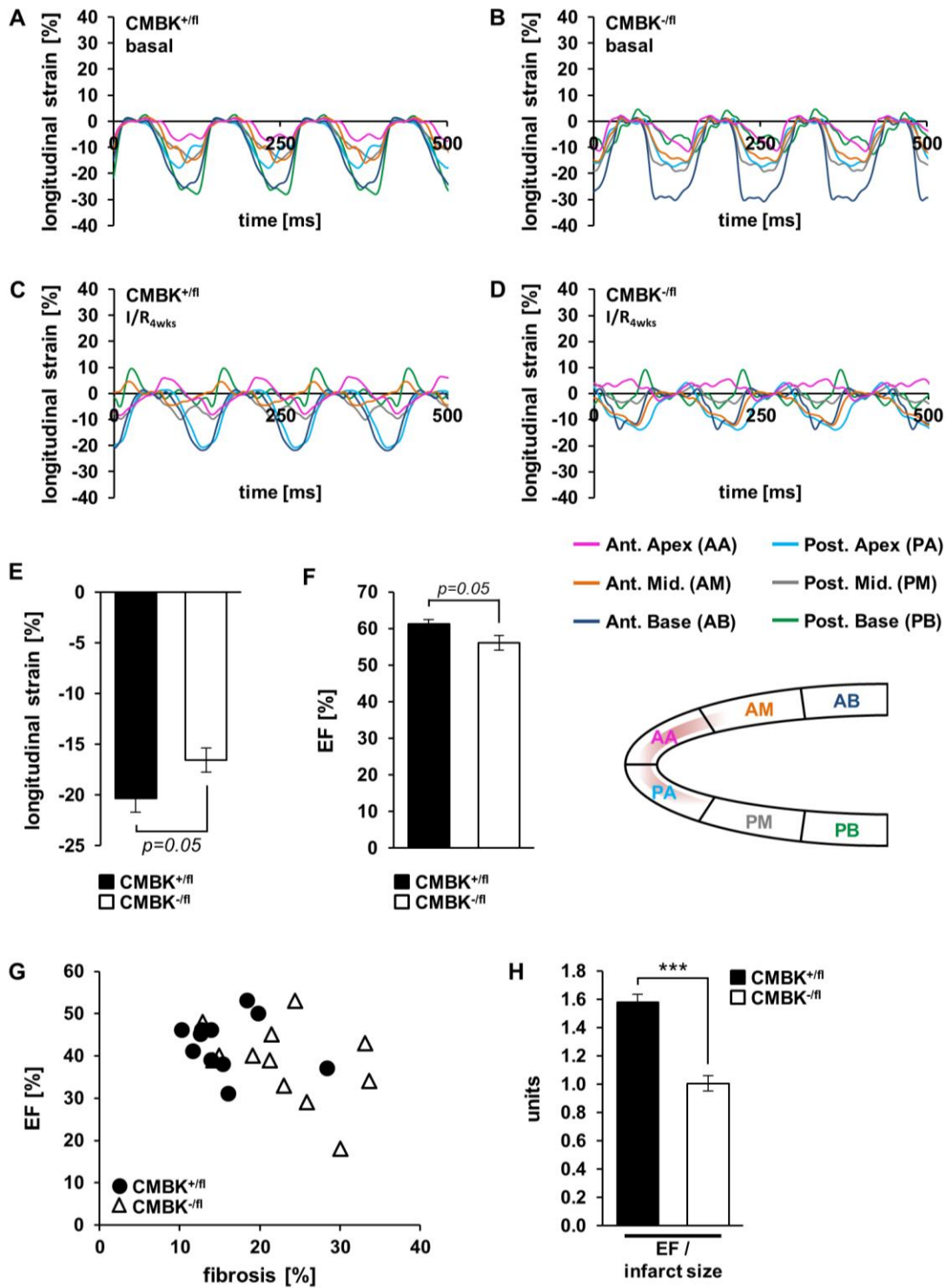


**Suppl. Fig. 14:** *cGKI* is detectable in the mitochondrial protein fraction purified from *BK*<sup>+/+</sup> and *BK*<sup>-/-</sup> cardiomyocytes

(A) Representative immunoblot showing expression of cGKI protein in cardiomyocyte mitochondria (CMM) and whole heart lysates (HL) from BK-WT (*BK*<sup>+/+</sup>) and BK-KO (*BK*<sup>-/-</sup>) mice using a custom-made antibody. By co-detection of α-tubulin and hsp60 the purity of the mitochondrial protein fraction as well as the enrichment of the matrix protein in the mitochondrial fraction were verified. (B) Purity of isolated mitochondria was further confirmed using antibodies that specifically identified mitochondrial proteins (NADH-ubiquinone oxidoreductase subunit of complex I and cytochrome c oxidase (COX IV)) in the mitochondrial protein fraction obtained from cardiomyocyte mitochondria, whereas cytosolic proteins such as α-tubulin and GAPDH or the β<sub>1</sub>-adrenoreceptor (β<sub>1</sub>-AR) that was used as a plasma membrane marker could not be detected in the respective fraction. Apparently, complex I and COX IV proteins were enriched in the mitochondrial protein fraction from isolated CMs while β<sub>1</sub>-AR and α-tubulin could only be detected in whole HL. (C) *Vice versa*, the cytosolic protein fractions contained GAPDH but not complex I proteins from the inner membrane of mitochondria.



**Suppl. Fig. 15:** Flowchart of the patch-clamp experiments (see Supplemental Methods for further details).

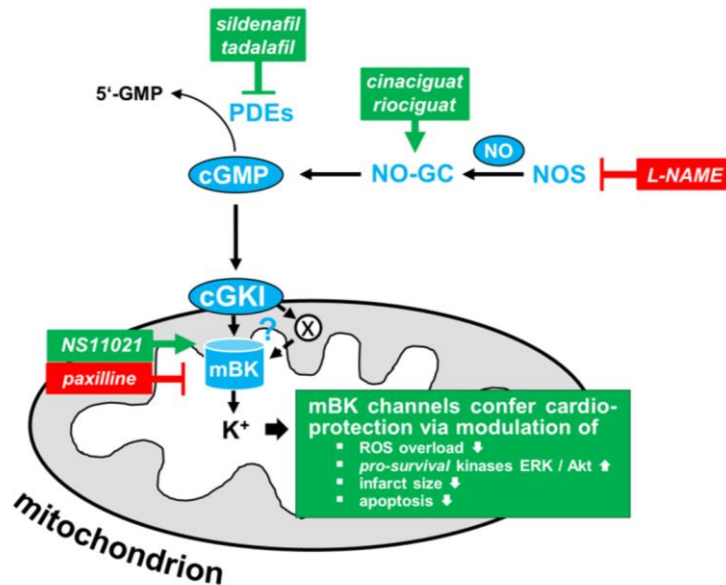


**Suppl. Fig. 16: Abnormal strain curves of CMBK-KO hearts following myocardial infarction**

Representative echocardiographic recordings of the longitudinal strain (%) of (A) CMBK-CTR (CMBK<sup>+fl</sup>) and (B) CMBK-KO mice (CMBK<sup>-fl</sup>) under basal conditions and after 30 min ischemia followed by 4 weeks of reperfusion (I/R<sub>4wks</sub>) in (C) CMBK<sup>+fl</sup> and (D) CMBK<sup>-fl</sup> mice. (E) Average longitudinal strain was slightly reduced in CMBK<sup>-fl</sup> compared to littermatched controls under basal conditions (n=8 per genotype). (F) Vevo Strain analysis displayed a reduced ejection fraction (EF, %) in CMBK<sup>-fl</sup> hearts under basal conditions (n=8 per

genotype), which is in agreement with the conventional examination (Fig. 3B). (G) Amount of fibrosis (%) plotted against the ejection fraction (EF, %) in CMBK<sup>+fl</sup> and CMBK<sup>-fl</sup> mice 28 days after MI. (H) The ratio between the post-MI EF and the acute infarct size was significantly decreased in CMBK<sup>-fl</sup> (n=12) as compared to CMBK<sup>+fl</sup> (n=11) mice. Data in (E), (F) and (H) were analyzed using the Student's t-test and presented as means ± SEM with \*\*\*p<0.001.

**A** Cardioprotective signaling during I/R involving mitochondrial BK channels in the cardiomyocyte



**B** Open questions of the present study

1. The K<sup>+</sup> influx via mBK at I/R may oppose the mitochondrial overload with Ca<sup>2+</sup> as well as ROS production.<sup>13, 21, 22</sup>
2. Opening of mBK may lead to a mild uncoupling of the ETC as a possible downregulator of ROS production. In addition there may also be cardioprotection via PKC.<sup>23-25</sup> PKC, by recruiting additional pro-survival kinases such as ERK and Akt of the RISK pathway and phosphorylation of GSK3β, may inhibit the opening of the mPTP.<sup>23, 26-28</sup>
3. mBK channels were implicated in mitochondrial volume control and in altering the proton electrochemical potential gradient across the mitochondrial inner membrane to confer cardioprotection.<sup>13, 29</sup>

**Suppl. Fig. 17:** Putative signaling mechanisms during ischemia and reperfusion involving the second messenger cGMP and mitochondrial BK channels

(A) Pharmacological activation of the cGMP/cGKI pathway affords cardioprotection via mitochondrial BK channels (mBK) located at the inner mitochondrial membrane of CMs. (B) Putative downstream signaling mechanisms leading to cardioprotection. Abbreviations used: NOS: nitric oxide synthase; NO: nitric oxide; NO-GC: soluble guanylyl cyclase; PDEs: phosphodiesterases; cGMP: cyclic guanosine 3',5'-monophosphate; cGKI: cGMP-dependent protein kinase type I; mBK: mitochondrial BK channel; ROS: reactive oxygen species; ETC: electron transport chain; PKC: protein kinase C; GSK3β: glycogen synthase kinase 3 beta; mPTP: mitochondrial permeability transition pore.

## **SUPPLEMENTAL REFERENCES**

1. Methner C, Lukowski R, Grube K, Loga F, Smith RA, Murphy MP, Hofmann F and Krieg T. Protection through postconditioning or a mitochondria-targeted S-nitrosothiol is unaffected by cardiomyocyte-selective ablation of protein kinase G. *Basic Res Cardiol.* 2013;108:337.
2. Schwanke U, Konietzka I, Duschin A, Li X, Schulz R and Heusch G. No ischemic preconditioning in heterozygous connexin43-deficient mice. *Am J Physiol Heart Circ Physiol.* 2002;283:H1740-1742.
3. Eckle T, Grenz A, Kohler D, Redel A, Falk M, Rolauffs B, Osswald H, Kehl F and Eltzschig HK. Systematic evaluation of a novel model for cardiac ischemic preconditioning in mice. *Am J Physiol Heart Circ Physiol.* 2006;291:H2533-2540.
4. Imlach WL, Finch SC, Dunlop J, Meredith AL, Aldrich RW and Dalziel JE. The molecular mechanism of "ryegrass staggers," a neurological disorder of K<sup>+</sup> channels. *J Pharmacol Exp Ther.* 2008;327:657-664.
5. Lai MH, Wu Y, Gao Z, Anderson ME, Dalziel JE and Meredith AL. BK channels regulate sinoatrial node firing rate and cardiac pacing in vivo. *Am J Physiol Heart Circ Physiol.* 2014;307:H1327-1338.
6. Methner C, Buonincontri G, Hu CH, Vujic A, Kretschmer A, Sawiak S, Carpenter A, Stasch JP and Krieg T. Riociguat reduces infarct size and post-infarct heart failure in mouse hearts: insights from MRI/PET imaging. *PLoS One.* 2013;8:e83910.
7. Salloum FN, Das A, Samidurai A, Hoke NN, Chau VQ, Ockaili RA, Stasch JP and Kukreja RC. Cinaciguat, a novel activator of soluble guanylate cyclase, protects against ischemia/reperfusion injury: role of hydrogen sulfide. *Am J Physiol Heart Circ Physiol.* 2012;302:H1347-1354.
8. Salloum FN, Chau VQ, Hoke NN, Abbate A, Varma A, Ockaili RA, Toldo S and Kukreja RC. Phosphodiesterase-5 inhibitor, tadalafil, protects against myocardial ischemia/reperfusion through protein-kinase g-dependent generation of hydrogen sulfide. *Circulation.* 2009;120:S31-36.
9. Gotz KR, Sprenger JU, Perera RK, Steinbrecher JH, Lehnart SE, Kuhn M, Gorelik J, Balligand JL and Nikolaev VO. Transgenic mice for real-time visualization of cGMP in intact adult cardiomyocytes. *Circ Res.* 2014;114:1235-1245.
10. Lukowski R, Rybalkin SD, Loga F, Leiss V, Beavo JA and Hofmann F. Cardiac hypertrophy is not amplified by deletion of cGMP-dependent protein kinase I in cardiomyocytes. *Proc Natl Acad Sci U S A.* 2010;107:5646-5651.
11. Straubinger J, Schottle V, Bork N, Subramanian H, Dunnes S, Russwurm M, Gawaz M, Friebe A, Nemer M, Nikolaev VO and Lukowski R. Sildenafil Does Not Prevent Heart Hypertrophy and Fibrosis Induced by Cardiomyocyte Angiotensin II Type 1 Receptor Signaling. *J Pharmacol Exp Ther.* 2015;354:406-416.
12. Bauer M, Cheng S, Jain M, Ngoy S, Theodoropoulos C, Trujillo A, Lin FC and Liao R. Echocardiographic speckle-tracking based strain imaging for rapid cardiovascular phenotyping in mice. *Circ Res.* 2011;108:908-916.
13. Soltysinska E, Bentzen BH, Barthmes M, Hattel H, Thrush AB, Harper ME, Qvortrup K, Larsen FJ, Schiffer TA, Losa-Reyna J, Straubinger J, Kniess A, Thomsen MB, Bruggemann A, Fenske S, Biel M, Ruth P, Wahl-Schott C, Boushel RC, Olesen SP and Lukowski R. KCNMA1 encoded cardiac BK channels afford protection against ischemia-reperfusion injury. *PLoS One.* 2014;9:e103402.
14. Frezza C, Cipolat S and Scorrano L. Organelle isolation: functional mitochondria from mouse liver, muscle and cultured fibroblasts. *Nat Protoc.* 2007;2:287-295.
15. Kicinska A, Augustynek B, Kulawiak B, Jarmuszkiewicz W, Szewczyk A and Bednarczyk P. A large-conductance calcium-regulated K<sup>+</sup> channel in human dermal fibroblast mitochondria. *Biochem J.* 2016;473:4457-4471.
16. Bednarczyk P, Wieckowski MR, Broszkiewicz M, Skowronek K, Siemen D and Szewczyk A. Putative Structural and Functional Coupling of the Mitochondrial BKCa Channel to the Respiratory Chain. *PLoS One.* 2013;8:e68125.
17. Cocheme HM, Quin C, McQuaker SJ, Cabreiro F, Logan A, Prime TA, Abakumova I, Patel JV, Fearnley IM, James AM, Porteous CM, Smith RA, Saeed S, Carre JE, Singer M, Gems D, Hartley RC, Partridge L and Murphy MP. Measurement of H<sub>2</sub>O<sub>2</sub> within living *Drosophila* during aging using a ratiometric mass spectrometry probe targeted to the mitochondrial matrix. *Cell Metab.* 2011;13:340-350.

18. Chouchani ET, Methner C, Nadtochiy SM, Logan A, Pell VR, Ding S, James AM, Cocheme HM, Reinhold J, Lilley KS, Partridge L, Fearnley IM, Robinson AJ, Hartley RC, Smith RA, Krieg T, Brookes PS and Murphy MP. Cardioprotection by S-nitrosation of a cysteine switch on mitochondrial complex I. *Nat Med.* 2013;19:753-759.
19. Sausbier M, Hu H, Arntz C, Feil S, Kamm S, Adelsberger H, Sausbier U, Sailer CA, Feil R, Hofmann F, Korth M, Shipston MJ, Knaus HG, Wolfer DP, Pedroarena CM, Storm JF and Ruth P. Cerebellar ataxia and Purkinje cell dysfunction caused by Ca<sup>2+</sup>-activated K<sup>+</sup> channel deficiency. *Proc Natl Acad Sci U S A.* 2004;101:9474-9478.
20. Sausbier M, Arntz C, Bucurenciu I, Zhao H, Zhou XB, Sausbier U, Feil S, Kamm S, Essin K, Sailer CA, Abdullah U, Krippeit-Drews P, Feil R, Hofmann F, Knaus HG, Kenyon C, Shipston MJ, Storm JF, Neuhuber W, Korth M, Schubert R, Gollasch M and Ruth P. Elevated blood pressure linked to primary hyperaldosteronism and impaired vasodilation in BK channel-deficient mice. *Circulation.* 2005;112:60-68.
21. Kang SH, Park WS, Kim N, Youm JB, Warda M, Ko JH, Ko EA and Han J. Mitochondrial Ca<sup>2+</sup>-activated K<sup>+</sup> channels more efficiently reduce mitochondrial Ca<sup>2+</sup> overload in rat ventricular myocytes. *Am J Physiol Heart Circ Physiol.* 2007;293:H307-313.
22. Sato T, Saito T, Saegusa N and Nakaya H. Mitochondrial Ca<sup>2+</sup>-activated K<sup>+</sup> channels in cardiac myocytes: a mechanism of the cardioprotective effect and modulation by protein kinase A. *Circulation.* 2005;111:198-203.
23. Costa AD and Garlid KD. Intramitochondrial signaling: interactions among mitoKATP, PKCepsilon, ROS, and MPT. *Am J Physiol Heart Circ Physiol.* 2008;295:H874-882.
24. Costa AD, Pierre SV, Cohen MV, Downey JM and Garlid KD. cGMP signalling in pre- and post-conditioning: the role of mitochondria. *Cardiovasc Res.* 2008;77:344-352.
25. Stowe DF, Aldakkak M, Camara AK, Riess ML, Heinen A, Varadarajan SG and Jiang MT. Cardiac mitochondrial preconditioning by Big Ca<sup>2+</sup>-sensitive K<sup>+</sup> channel opening requires superoxide radical generation. *Am J Physiol Heart Circ Physiol.* 2006;290:H434-440.
26. Hausenloy DJ, Tsang A and Yellon DM. The reperfusion injury salvage kinase pathway: a common target for both ischemic preconditioning and postconditioning. *Trends Cardiovasc Med.* 2005;15:69-75.
27. Hausenloy DJ and Yellon DM. Reperfusion injury salvage kinase signalling: taking a RISK for cardioprotection. *Heart Fail Rev.* 2007;12:217-234.
28. Miura T and Tanno M. The mPTP and its regulatory proteins: final common targets of signalling pathways for protection against necrosis. *Cardiovasc Res.* 2012;94:181-189.
29. Aon MA, Cortassa S, Wei AC, Grunnet M and O'Rourke B. Energetic performance is improved by specific activation of K<sup>+</sup> fluxes through K(Ca) channels in heart mitochondria. *Biochim Biophys Acta.* 2010;1797:71-80.